Master's Thesis

Towards Functionalised Bacterial Cellulose: Assessing Coexistence in a SCOBY-based *K. sucrofermentans - S. cerevisiae* Coculture

Author: Iris Gormezano Kasuto

Supervisor: Pieter Candry

Examiner: Stefan Hoffman

Wageningen University & Research

Systems and Synthetic Biology

MSc Environmental Biotechnology

08 January 2026

Abstract

Bacterial cellulose (BC) is an emerging biobased material with high purity, tunable structure and potential for functionalisation through proteins. However, conventional monoculture processes with *Komagataeibacter* spp. face challenges in limited genetic toolbox, toxic byproduct production, and the emergence of cellulose negative: Cel^- mutants. This work explored a coculture strategy between *Komagataeibacter sucrofermentans* and an engineered *Saccharomyces cerevisiae* IMX1812 strain as a first step towards a stable synthetic-SCOBY (Syn-SCOBY) platform for BC functionalisation. Literature demonstrated that the supplementation of ethanol at optimal amounts increased productivity of BC production. Here, yeast is proposed as a promising candidate as yeast naturally ferments sugars to ethanol in kombucha cultures. Engineered yeast restricted to consuming maltose was used, with glucose reserved for *Komagataeibacter*. Growth kinetics data of *K.sucrofermentans*, and respiratory and fermentative *S.cerevisiae* IMX1812 on gradients of relevant coculture substrates were obtained, thereby providing a quantitative basis for future strain engineering and bioprocess optimisation of functionalised BC systems. Furthermore, the effect of a fermentative versus respiratory yeast and prolonged agitation on coexistence and BC synthesis was investigated. It was determined that coexistence between the two strains is possible, while revealing that acid toxicity and the genetic instability of *Komagataeibacter* are important design constraints for future work.

Keywords and Abbreviations: bioeconomy, biomaterials, bacterial cellulose (BC), acetic acid bacteria (AAB), synthetic Symbiotic Culture of Bacteria and Yeast (Syn-SCOBY), synthetic community (SynCom), synthetic biology (SynBio), coculture, cross-feeding, programmable materials, cellulose-negative phenotypes of *Komagataeibacter* (Cel^-) mutants)

1 Acknowledgements

This thesis was carried out as part of a larger project that participated in the 2025 iGEM competition. I was a part of the Wageningen University & Research team BCoated!. The intersectoral nature of iGEM provided an invaluable learning experience to me, offering a new and more realistic perspective on the complexity that plays into the transition to a bioeconomy, and on the role of scientists collaborating with other stakeholders in this process.

I would like to thank all of my teammates, Andra Stoica, Anirudhn Puvvada, Camile van Harmelen, Daan van den Bor, Jochem Feith, Niels van de Sande, Rick Markus, Tifara Elaine Trisna, Varsha Saravanan, Yoerik van den Bergh for everything they taught me along the way. I also thank all supervisors and laboratory technicians involved in the project for their guidance and support.

Contributions.

The glucose-deficient strain *Saccharomyces cerevisiae* IMX1812 was kindly provided by Pascale Daran Lapujade and Delft University of Technology. The wild-type *S. cerevisiae* and Δ *S. cerevisiae* strains were provided by Camile Harmelen. Pieter Candry provided scientific supervision and the R script used for growth-curve analysis. Koen Smith and Sam Hoogarts offered expertise when executing the protocols. The illustrations in Figure 3 and Figure 4 were drawn by Andra Stoica. Additional supervision was provided by Robert Smith.

Contents

2 Introduction

2.1 Transition from petrochemicals to biomaterials with SynBio

Global warming has now exceeded the 1.5°C limit set by the United Nations Framework Convention on Climate Change (Paris Agreement, 2015) and several of the planetary boundaries have reached their predefined tipping points. [34]. To mitigate this, Europe has passed the Green Deal (2019) growth strategy to transform the EU into a resource-efficient and competitive economy. The European bioeconomy policies, including the climate pact and laws that contribute to the Green Deal, state that carbon sequestration and material substitution of fossil-based products such as plastics and textiles, can generate significant carbon savings and achieve a 55% reduction by 2030 [3].

Synthetic biology (SynBio) has emerged as a key field in enabling this transition from petrochemicals to biobased and biodegradable materials and rethinking the conventional production methods. More recently, the value of exploiting inherent features within biology to program and adjust materials for their specific use has been particularly highlighted [18]. For a long time in biotechnology, the focus has been on model organisms that are easy to grow, access, and modify genetically. However, for many applications, it may be more efficient to exploit the native abilities of nonmodel organisms that specialise in certain functions, such as synthesising biopolymers. Polymer-producing bacteria have the potential to become especially prominent in the accelerated use of biomaterials because the process can be modified to enhance the utility of the polymer, such as sensing and responding, or with functional proteins. Such examples include biobased polymers like polyhydroxyalkanoates (PHA), alginate, and bacterial cellulose (BC) [33]. These polymers are of special interest because they can be produced at commercial scale from microbial growth on waste streams [35], further complying with the principles of a bioeconomy.

2.2 Bacterial cellulose (BC) is highly tunable for various uses in diverse sectors but comes with limitations

Cellulose is an abundant, renewable and biodegradable biopolymer that is already widespread in major industrial sectors, including paper and packaging, textiles, construction materials and medicine [5]. However, currently, cellulose is predominantly sourced from lignocellulosic biomass, where cellulose is a part of a matrix composed of lignin, hemicellulose and other components. Recovering plant-derived cellulose, therefore, requires purification of these other components through intensive energy and chemical pulping and bleaching at high temperatures, which reduces the overall sustainability of the process. The large scale production of plant cellulose also depends on forestry, which implies land

use and potential deforestation. In contrast, bacterial cellulose (BC) consists of the same β-1,4-glucan chains as plant cellulose but is synthesised extracellularly by bacteria as a highly pure cellulose structure that is free of lignin and hemicellulose forming a highly crystalline, nanofibrillar network. As a result, BC usually requires only mild downstream treatments, such as alkaline washing to remove cells. Moreover, BC can be produced in controlled bioreactors using various substrates, including industrial waste streams, supporting circular bioeconomy strategies [26].

Beyond sourcing from different substrates, BC also has a wide range of potential applications. BC can be used as leather replacement in the textile industry [31], membranes in batteries [40], as wound dressing and drug delivery in the medical industry [37], a stabilizer and delivery medium in the cosmetic industry [25], additive/stabilizer or packaging in the food industry [38], acoustic absorbent in high end acoustics [16], and more. The attractiveness of its use in so many different sectors can be attributed to its high and flexible/tunable biodegradability, crystallinity, porosity, mechanical/tensile strength, water retention, and high purity and biocompatibility ([15]). Moreover, controlling the properties of BC matrices can be achieved simply by changing operation conditions such as pH, temperature, agitation, and substrate composition [20]. More advanced approaches include genetically engineering certain genes [7], further customisation with dyes, or functionalisation by attaching proteins by fusion with the cellulose-binding-domain (CBD). Such approaches can, for instance, bring about antimicrobial properties and biosensor abilities. The matrix can even be used as a controlled delivery system of proteins, drugs, enzymes, or chemicals by adjusting the porosity and biodegradability desirably [32]. Overall, a range of approaches is available to tune BC properties to the application at hand.

The research on BC production has primarily focused on *Komagataeibacter* sp., previously known as *Gluconacetobacter* and *Acetobacter*, due to the high level of extracellular BC synthesis. The model organisms that have been used for commercial applications of BC include *K.xylinus*, *K.hansenii*, *K.sucrofermentans* and *K. rhaeticus*. Thanks to combined efforts, these organisms have been explored in terms of their main carbon metabolism [17] , BC biosynthesis pathways and their phylogeny [4], and genomic sequence [38] [4] ([23]. Although modular genetic toolkits for these bacteria are emerging, and basic cloning methods such as Golden Gate assembly (GGA) together with parts like promoters, fusion tags and reporter proteins have been described [12], these resources are still minimal compared with those available for standard SynBio hosts such as *Escherichia coli* and *Saccharomyces cerevisiae*. This underdeveloped toolbox currently limits the engineerability of BC production, hindering the ability of enhancing the yield and versatility of BC with SynBio.

In addition to these genetic limitations, the native *Komagataeibacter* carbon metabolism further constrains the BC yield. At the metabolic level, BC yield

in *K. sucrofermentans* is strongly influenced by how glucose flux is partitioned between periplasmic oxidation, energy generation and cellulose polymerisation (Figure 1). Glucose can either be imported into the cytoplasm and converted via UDP-glucose into cellulose, or it can be incompletely oxidised in the periplasm by PQQ-dependent dehydrogenases such as glucose dehydrogenase (GDH) to gluconate and keto-gluconates, with the released electrons feeding the electron transport chain and driving ATP formation [22]. The assimilation of glucose for energy also generates acidic byproducts (i.e., acetic acid and gluconic acid) which can become toxic when they are released into the medium and lead to a pH reduction. Because a substantial amount of glucose can be diverted towards periplasmic oxidation and acidic byproducts, BC production in this species is often limited by both its energy metabolism and the accumulation of gluconate and acetate. When ethanol is present in the medium, it is oxidised in the periplasm by PQQ-dependent alcohol and aldehyde dehydrogenases to acetaldehyde and acetate, which can be further converted to acetyl-CoA and fully oxidised through the tricarboxylic acid (TCA) cycle, again contributing to ATP generation [41] (Figure 1)

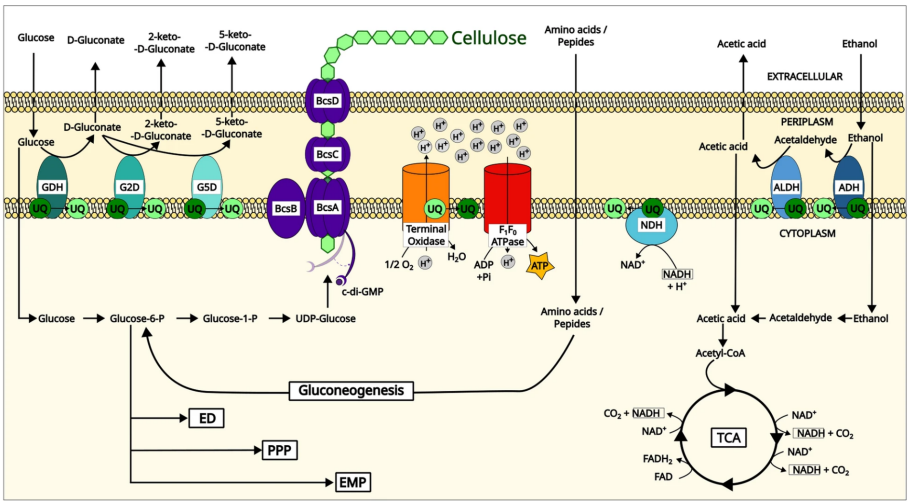

Figure 1: **Overview of glucose and ethanol metabolism in *Komagataeibacter sucrofermentans* and their links to bacterial cellulose (BC) synthesis.** In the periplasm, glucose can be incompletely oxidised by PQQ-dependent dehydrogenases (GDH, G2DH, G5DH) to gluconate and ketogluconates, transferring electrons to ubiquinone (UQ) and feeding the electron transport chain for ATP synthesis. Alternatively, glucose can be imported, converted via UDP-glucose and polymerised by the cellulose synthase complex (BcsA–D) into BC. Ethanol is oxidised by PQQ-dependent alcohol and aldehyde dehydrogenases (ADH, ALDH) to acetaldehyde and acetate; these metabolites can be assimilated to acetyl-CoA and fully oxidised via the TCA cycle, also contributing to ATP generation. Ethanol supplementation therefore increases energy supply and can suppress periplasmic oxidation of glucose to gluconate, shifting carbon towards BC formation. Reproduced from "Enhanced bacterial cellulose production in Komagataeibacter sucrofermentans: impact of different PQQ-dependent dehydrogenase knockouts and ethanol supplementation," by P. Montenegro-Silva, T. Ellis, F. Dourado, M. Gama, and L. Domingues, 2024, Biotechnology for Biofuels and Bioproducts, 17(1), Article 35 [22]

Several studies suggest that carefully titrated ethanol supplementation can partially relieve this energetic bottleneck and increase BC yield. Naritomi et al. reported that adding 1% (v/v) ethanol to the medium enhanced BC production, whereas concentrations above 1.5% reduced BC production due to excessive acetate formation [6]. Montenegro Silva et al. further showed that ethanol oxidation enhances proton translocation and ATP generation and, at the same time, suppresses GDH-mediated oxidation of glucose to gluconic acid in the periplasm [22]. When PQQ-dependent GDH was knocked out, gluconic acid production ceased and BC titres increased by 5.77-fold; this improvement was reduced to 2.26-fold at the optimal ethanol concentration, indicating that the positive effect

of ethanol on BC yield can partly be attributed to the combined effects of additional energy generation and reduced carbon loss to gluconate [22]. In addition to these metabolic constraints, BC production is further limited by reactor configuration and oxygen transfer, which create a trade-off between pellicle quality and process scalability, as discussed in the following paragraph.

Another well-known limitation in bacterial cellulose production is the trade-off between obtaining high quality BC pellicles at the air-liquid interface with static cultivation vs. providing consistent oxygen supply throughout the reactor and obtaining pellets (Figure 1). Poor oxygen diffusion limits industrial viability for the obligately aerobic *Komagataeibacter* species. Conversely, agitated bioreactor systems improve oxygen and nutrient transfer, but comes with its own shortcomings (Figure 1) [10]. The pellicle shape allows for direct use in these applications with minimal processing, whereas a pellet form would require significant re-processing into a film or scaffold, adding complexity and cost.

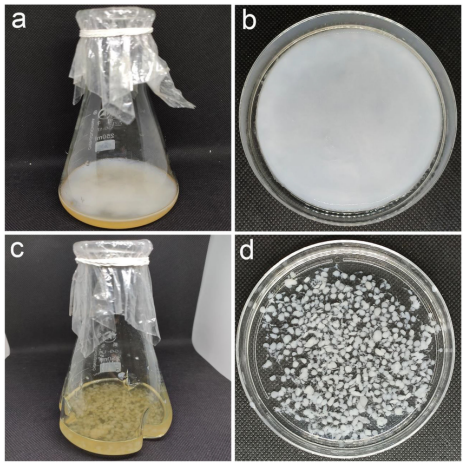

Figure 2: **BC produced via static and agitated fermentation.** a. BC pellicle formed at the air-liquid interface of the broth in a static fermentation. b. The purified BC pellicle with uniform texture c. BC pellets distributed throughout the broth in an agitated fermentation. d. The purified BC pellets with irregular shapes. Reproduced from "Industrial-scale production and applications of bacterial cellulose. C. Zhong, 2020, Frontiers in Bioengineering and Biotechnology, 8, Article 605374 [43]

2.3 A Coculture Approach to Address the Limitations of BC Production

While the engineering of BC producers to enhance yield or customise the material is difficult, coculturing these bacteria with model SynBio organisms that

have more readily available engineering pipelines presents a promising alternative. For material functionalisation, the coculture partner can secrete dyes, enzymes or proteins that will attach to the matrix, or provide/take up beneficial/toxic compounds from the medium. This approach has been considered for BC biomanufacturing before. One such study by Zhou et al. (2025) describes the one pot production of coloured BC by introducing *E.coli* into the consortium with *K. xylinus* for natural colorant synthesis to achieve multicolored BC [44]. Similarly, inspired by the symbiotic fermentation culture starter for kombucha (i.e., Symbiotic culture of bacteria and yeast, or,SCOBY), Gilbert et al. (2021) incorporated engineered *S. cerevisiae* with *K. rhaeticus* to yield a synthetic SCOBY (Syn-SCOBY) and add functional traits to the cellulose matrix. Engineered *S. cerevisiae* has been used in Syn-SCOBY systems to secrete enzymes directly into the cellulose matrix, enabling the autonomous growth of catalytic materials whose activity can be tuned by genetic design. In addition, cellulose matrices have been produced with *S. cerevisiae* embedded within the growing network, creating a living material that can respond to chemical or optical signals [11]. This paves the way for potential uses of the Syn-SCOBY platform to produce BC that, for example, senses and degrades environmental pollutants, through the attachment of engineered functional proteins and the release of active compounds (Figure 3). This study proposes a similar coculture strategy with *K. sucrofermentans* and *S. cerevisiae* as a modular streamline for efficient and scalable functionalised BC biomanufacturing.

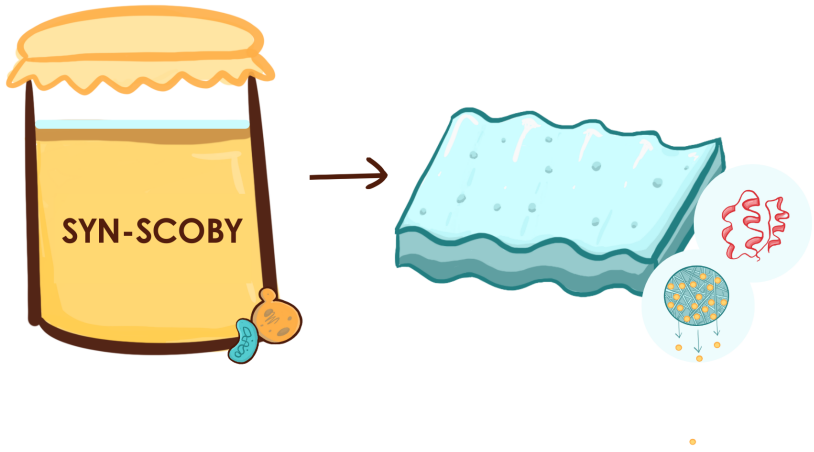

Figure 3: **Syn-SCOBY approach to functionalise BC** A synthetic model SCOBY culture can be cultivated with *K.sucrofermentans* and *S.cerevisiae* to expand the functionality of the material. *S.cerevisiae* can be engineered to secrete proteins on the matrix that can sense environmental stimuli and release active compounds.

High production costs and low yield were identified as the main limitations to overcome in reaching industrially relevant scales of BC production. To solve this, studies presented in Table 1 have carried out a coculture strategy of *Komagataeibacter* species (sp.) to improve the BC yield.

Table 1: Reported coculture strategies with *Komagataeibacter* (*Gluconacetobacter*) species to improve bacterial cellulose production. Summarized from [1]

Cellulose-producing strain	**Coculture partner (strain)**	**Main outcome vs. monoculture**	**Study**
Gluconacetobacter xylinus st-60-12	*Lactobacillus mali* st-20	3-fold increase in BC production compared to *G. xylinus* st-60-12 monoculture.	(Seto et al., 2006)
Gluconacetobacter hansenii ATCC 23769	*Escherichia coli* ATCC 700728	10.8% increase in BC yield and improved mechanical properties compared to *G. hansenii* ATCC 23769 monoculture.	(Liu & Catchmark, 2019)
Komagataeibacter xylinus gcd gene-disrupted strain (encoding glucose dehydrogenase, GDH), derived from *K. xylinus* CGMCC2955	*Bacillus cereus* (isolated in this study)	BC yield increased from 1.2 g/L to 4.4 g/L in corn stover enzymatic hydrolysate (approximately 3.7-fold increase).	(W. Li et al., 2023)
Komagataeibacter hansenii ATCC 23769	*Aureobasidium pullulans* ATCC 201253	Improved mechanical properties of BC without affecting production yield.	Liu & Catchmark, 2019
Komagataeibacter xylinus MS2530	Yeast strains: *Pichia pastoris* MDC 10178, *Pichia fermentans* MDC 10169, *Kluyveromyces marxianus* MDC 10081	Fermentation time reduced from 14 days to 7 days. Use of brewery spent yeast (BSY) medium without pretreatment or sterilization reduced medium cost (HS: \$5.52/L vs. BSY: \$0.13/L) and increased BC yield to 20.9 g/L in HS and 26.4 g/L in BSY.	(Paronyan et al., 2025)

In addition to improving the yield, Paronyan et al. (2025) considered minimizing the cost of production through the utilization of inexpensive cultivation feedstocks, such as recycled industrial waste, aligning with the principles of a circular bioeconomy. They have achieved this by employing the coculture strategy with *K.xylinus* and various yeast strains growing on brewery waste, which also reduced the fermentation time (Table 1). Gao et al. also highlighted the

importance of developing microbial platforms that can ferment mixed sugars simultaneously for reaching economical commercial level scales, and proposed to include yeast in cell factories for improved substrate co-utilization [9]. These cocultures may reduce fermentation time and increase BC yield through several, or combined, mechanisms. One such mechanism is division of labour, which allows different species to specialise on distinct tasks or substrates, so that no single organism carries the full metabolic burden. Another is where each partner can consumes different components of the medium, or convert inhibitory intermediates produced by the other, which reduces the accumulation of toxic by-products and helps relieve thermodynamic, redox, or pH bottlenecks. Together, these effects can mitigate the drawbacks associated with heavy gene overexpression, intermediate build-up and unfavourable reaction energetics, leading to higher overall productivity and improved yields [21].

Cocultures can be beneficial in a certain window of conditions for a certain amount of time. However, for the commercial relevance of the production process, it should be a robust coculture. Robustness can be defined as compositional or functional robustness. Compositional robustness refers to the ability of the community composition to return to its stable state upon perturbations, such as changes in pH, temperature, or media composition, or across batches. Functional robustness, on the other hand, would mean consistency in the BC yield and type of BC produced by this coculture. Within a synthetic coculture, the type and strength of interspecies interaction, relative fitness and growth rates of the species within the defined media, and operative conditions are important determinants of robustness. Combining strains can also provoke competitive or even antagonistic behaviour with unfavourable effects on process performance, particularly when species directly compete for the primary carbon and energy source. For biomanufacturing processes, it is therefore common to *aim* for cooperative relationships such as mutualism or commensalism, or at least to minimise direct resource competition. However, the idea that more cooperative interactions are always more robust or productive has recently been questioned. Still, especially in the cases of obligately cross-feeding mutualistic interactions, a tighter control of the interaction and desired production is facilitated. [13, 27, 14].

Here, considering all the limitations and background on cocultures of BC production, a design in which the *S.cerevisiae* is unable to transport and consume glucose (*S.cerevisiae* IMX1812) ([39] is proposed. With this approach, it is hypothesised that glucose in the medium can be primarily used for BC polymerisation. As mentioned before, providing ethanol to *K.sucrofermentans* is a potential strategy of repressing the conversion of glucose into gluconic acid by supplementing another path to gain ATP. Thus, the design further exploits the native fermentation activity of yeast to convert maltose (the main sugar source for the strain IMX1812) into ethanol. The effect of ethanol provided by the coculture partner on BC yield is further investigated compared to *Komagataeibacter sucrofermentans*. Self-metabolisation of ethanol by yeast was

inhibited through an induced mutation to its mitochondria (Figure 4). This thesis therefore presents a coculture between *K. sucrofermentans* and *S. cerevisiae* in which *S. cerevisiae* serves primarily as an engineerable chassis for future in situ BC functionalisation, while being restricted to maltose to avoid competition for glucose and simultaneously supplying ethanol that can support BC production. In contrast to the BC cocultures summarised in Table **??**, which mainly aim to improve productivity, substrate utilisation or mechanical properties, this design is hypothesised to establish a coculture that conserves BC yields comparable to a *Komagataeibacter* monoculture while facilitating the use of SynBio to functionalise BC.

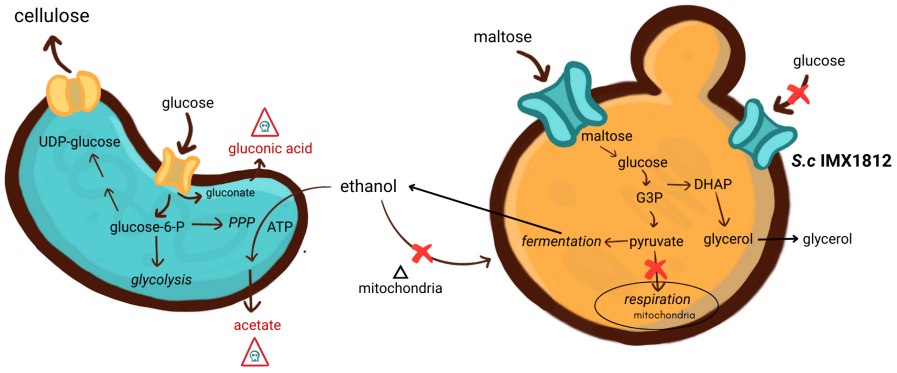

Figure 4: **Conceptual design of the engineered *Komagataeibacter sucrofermentans*–*Saccharomyces cerevisiae* co-culture and intended partnership for improved bacterial cellulose (BC) production.** *K.sucrofermentans* (left) takes up glucose and directs it to multiple pathways: central carbon metabolism (glucose-6-phosphate), generating ATP via glycolysis and the pentose phosphate pathway (PPP), while supplying UDP-glucose for bacterial cellulose biosynthesis. Glucose is also oxidised to gluconate (gluconic acid) in the periplasm, while ethanol is oxidised to acetaldehyde and then to acetic acid (acetate). Both gluconic acid and acetic acid can accumulate as extracellular byproducts of BC production (red), which reduces the pH and becomes toxic. The engineered *S. cerevisiae* strain IMX1812 (right) is designed to avoid competition for glucose and instead grows on maltose. Maltose is converted to glucose intracellularly and metabolized through glycolysis (via glyceraldehyde-3-phosphate, G3P, and dihydroxyacetone phosphate, DHAP) to pyruvate, which is directed to fermentative metabolism since respiratory metabolism is blocked through an induced mutation to the mitochondria. Fermentation results in secretion of ethanol and glycerol, with ethanol intended as a cross-fed substrate to support the energy metabolism of the bacterium, while glucose is reserved for cellulose synthesis. Ethanol reassimilation to *S.cerevisiae* is prevented through the loss of mitochondrial function.

3 Methods

3.1 Preparing the maltose positive and glucose negative *S. cerevisiae* IMX1812 $\rho-$ strain

For this consortium, the yeast partner should not consume glucose, nor reassimilate ethanol from the medium. The glucose-deficient *S.cerevisiae* IMX1812 strain was obtained from Pascale Daran-Lapujade from the Industrial Biotechnology Department of Delft University [39]. The history of this strain can be found in the Appendix7.1. This strain was prepared using CRISPR/SPCas9 to delete all 21 hexose transporters from an *S.cerevisiae* within the CEN.PK family. They report that, even upon prolonged cultivation, glucose consumption was still not observed, while the growth rate on maltose was the same as on glucose, independent of the presence of hexose transporters. Obtaining this strain was vital since glucose consumption by the yeast strain would result in competition against the acetic acid bacteria (AAB), and one species could have outgrown the other.

In the design of the coculture, yeast should only produce but never reassimilate and consume ethanol. To obtain this, mitochondrial function was knocked out to yield a $\rho-$ yeast strain. Ethidium bromide (EtBr) is an agent that induces respiratory deficiency through a mutation that causes loss of function of the cytoplasmic factor p. This mutation has is known to cause complete loss of mitochondrial DNA (mtDNA). We first inoculated *S. cerevisiae* IMX1812 in 3 mL YPM (6.8 g/L maltose) medium for around 3 hours. Then, a drop of the liquid culture was transferred to a YPM plate with 0.04 mg/mL EtBr. The plate was grown for 2 days in the 30°C incubator. The plate was scraped with an inoculation loop, focussing on colonies that are the roundest and smallest. Colonies were transferred to another YPM EtBr plate to grow until new colonies are observed (2.5-3 days). This process was repeated once more, and then the final (3rd) plate was used as the stamp for replica plating on YPG (YEP and 2% w/v glycerol medium) and YPM (YEP and 0.68% w/v maltose medium) plates with duplicates. By overlaying both the duplicates for the YPG and YPM plates on top of each other, $\rho-$ colonies could be identified, i.e., growth on YPM but not on YPG. The same was performed for *S.cerevisiae* CENPK113-7D with YPD instead of YPM to assess the change in growth kinetics upon just the mitochondrial mutation (Figure 5).

3.2 Quantifying the Growth Kinetics of the SynCom Partners in Monocultures

As a benchmark to rationally design and interpret the coculture experiments, we performed monoculture growth experiments of both *K. sucrofermentans* and engineered *S. cerevisiae*. This allowed us to obtain a baseline for growth charac-

teristics and substrate tolerances of each organism independently. Additionally, it ensured that potential toxicities, metabolic preferences, and kinetic parameters were well understood before introducing the complexity of interactions within the co-culture. The growth kinetics of each partner in monoculture were characterised on coculture-relevant substrates: glucose, maltose, glycerol, gluconate, ethanol, and acetate. These compounds were either primary carbon sources in the coculture medium or expected byproducts of the partners' metabolism. Because the toxic effects of acetate and gluconate have been linked to medium acidification [22], we also assessed their combined effect. For gluconate, acetate, ethanol, and acetate–gluconate mixtures (with gluconate held constant), we tested a range of concentrations to evaluate the beneficial or inhibitory effects of these metabolites on each species (see Appendix 7.3 for the 96 WP layouts). We used these results to estimate the optimal duration of the precultures and initial inoculation densities for the coculture, or as a point of reference when assessing the outcomes of the coculture.

For *K.sucrofermentans*, a 3 mL preculture was made in YPD medium and grown for around 16 hours overnight at 30°C shaking at 250 rpm with 1% (v/v) cellulase enzyme from Trichoderma reesei ATCC 26921 (Sigma-Aldrich) to obtain a homogeneous preculture without flocs in the agitated culture. Then, the preculture was transferred to a sterile microcentrifuge tube and spun down for 12 minutes at 3200 g twice for washing. The supernatant was discarded and the sample was resuspended in 2% YPD. This cell suspension was diluted so that the starting OD was 0.01. The medium used for the preculture and resuspension in the case of *S.cerevisiae* was YPM (6.8 g/L maltose), and the washing step was skipped since the carryover does not effect the measurements. Assays were performed in flat-bottom 96-well microplates in technical triplicate. Each well contained a sample volume of 150 μL, and was covered with 50μL of mineral oil to avoid water evaporating during the run. To prevent interference of cellulose pellicle formation with OD measurements, cellulase from Trichoderma reesei (Sigma-Aldrich) was added to all K. sucrofermentans cultures to a final concentration of 1% (w/v). To determine the growth rates, optical density (OD600) was tracked in a 30 degrees double orbital, continuously shaking plate reader (BioTek, Agilent Industries) for 3 days and with 15 minute data point intervals.

An R script provided by Pieter Candry was translated to Python to obtain average growth rates and other parameters, and the plots were prepared using a script prepared by Rick Marcus where an Excel template is used as input. Both scripts can be shared upon request.

3.3 Coculturing *S.cerevisiae* IMX1812 and *K.sucrofermentans*

Coculture experiments were performed to assess the coexistence of S. cerevisiae IMX1812 and *K.sucrofermentans* and the effect of ethanol supplied by *S. cere-*

visiae IMX1812 on cellulose production in the absence of competition for glucose. The protocol was adapted from Gilbert et al., and the preculture duration, starting OD_{600}, and the inoculation density was modified according to the change in the WT average growth rate upon the mitochondrial mutation [11].

Two days before the start of the coculture, *K. sucrofermentans* was inoculated from agar plates into 15 mL YPD medium supplemented with 1 % (v/v) cellulase and inoculated in a 30 °C incubator shaking at 250 rpm. Then, *S. cerevisiae* IMX1812 was inoculated 38 hours (24 hours in original protocol) before the experiment into a 15 mL YPM medium and incubated under the same conditions. Right before the start of the coculture experiment, the *K.sucrofermentans* preculture was centrifuged at 3600 rpm for 12 minutes twice to remove the cellulase enzyme. The pellets were resuspended in fresh YPM medium and the OD_{600} was adjusted to 2.5. Yeast precultures were diluted to an OD_{600} of 0.02 (0.01 in the original protocol). Three culture conditions were set up in duplicates in 100 mL Erlenmeyer flasks fitted with sterile rubber stoppers equipped with a sterile needle and syringe to allow sampling without opening the flask or disturbing the cellulose pellet. The yeast monoculture control was prepared with YPM, and 1.6 mL of the preculture was added. The *Komagataeibacter* monoculture was prepared with YPD medium, and 2 mL of the preculture was added. Finally, the coculture was prepared with YPDM medium using the same dilution factors as the monocultures. These cultures were incubated in a static incubator at 30 °C for 4 days or until the cellulose pellicles at the air-liquid interface of the Erlenmeyers did not appear to grow anymore.

At the starting point, 500 µL was taken from each flask, and sampling was repeated after 90 min and then hourly during the first 24 h. At the end of the 4 day incubation, a final endpoint sample was collected. Each 500 µL sample was centrifuged at 3000 g for 12 minutes. Pellets and supernatants were transferred to fresh tubes and stored frozen for subsequent analysis. The supernatants were then used for analysis by high-performance liquid chromatography (HPLC) to quantify the glucose, maltose, acetate, and ethanol, and pellets were used to check the coexistence after 4 days.

3.4 Compositional HPLC analysis of the coculture of *S.cerevisiae* IMX1812 and *K.sucrofermentans* and checking coexistence

HPLC analysis was carried out in an AMINEX hpx 87H column a flow rate of 0.6 ml/min at 60°C with 8 mM sulphuric acid and 100 mM isobutyric acid as an internal standard. For the detection, the refractive index detector was used since the yeast extract and peptone gave unidentifiable sample peaks in the UV detection method. Our compounds of interest were glucose, maltose, acetate, and ethanol. Calibration curves were obtained from standards of 10, 5, 2, 1, 0.5, and 0.25 g/L for each compound of interest (Appendix7.5).

3.5 Washing and Freeze drying BC to compare production within monoculture vs coculture

After 4 days, cellulose pellicles were harvested from the surface of the monoculture and coculture flasks with tweezers. Each pellicle was briefly rinsed with demineralised (demi) water. Individual pellicles were then transferred into beakers containing sufficient demi water to fully submerge the BC with a magnetic stirrer. The samples were washed at 100 rpm for 5 minutes at room temperature. After this first wash, the water was discarded and replaced with fresh demi water, and the washing step was repeated for another 5 minutes under the same agitation conditions. After this, the wash water was replaced with 0.1 M NaOH solution. The beakers were placed on a heated magnetic stirrer, and the temperature was raised to 80 °C while maintaining agitation at 100 rpm. After 15 minutes, the NaOH solution was exchanged for fresh 0.1 M NaOH and incubation at 80 °C with stirring was continued until the BC sheets became translucent from its initial white color. The washed pellicles were first air-dried and then placed overnight in the freeze-dryer before weighing and calculate the yield on the next day.

3.6 Coculturing *S.cerevisiae* IMX1812 $\rho-$ and *K.sucrofermentans* (coculture 2)

For coculture 2, the coexistence of *K.sucrofermentans* with the $\rho-$ strain was assessed. The changes made to the prior protocol was that the yeast preculture was prepared at the same time as for the bacterium, and *K.sucrofermentans* preculture was adjusted to an OD_{600} of 2.0 instead of 2.5. The medium used for all cultures including the monocultures was also YPDM for this coculture. Since a cellulose pellicle was not observed upon 1.5 days, all triplicates for all conditions were reinoculated. The flasks were kept in the static incubator for 4 more days after this.

3.7 Assessing coexistence in coculture 2 between *K.sucrofermentans* and *S.cerevisiae* IMX1812 $\rho-$

To assess whether both consortium partners' coexistence persisted during coculture 2, selective plating on YPDM media was used; supplemented with cycloheximide to select for *S.cerevisiae* IMX1812 $\rho-$, and with chloramphenicol to select for *K.sucrofermentans* since it contained the antibiotic resistance marker. Three plate types were prepared: A YPDM as a control where both strains are expected to be observed, (ii) YPDM supplemented with cycloheximide, and (iii) YPDM supplemented with chloramphenicol. For the cycloheximide plates, a filter-sterilised stock solution (25 µg dissolved in 5 mL 96% (v/v) ethanol; Sigma-Aldrich, code 01810-1G) was added at 150 µL per 15 mL YPDM plate

just before pouring. For the chloramphenicol plates, YPDM agar was supplemented with chloramphenicol to a final concentration of 185 µg/mL to select for *K. sucrofermentans*. To verify the expected colony appearance of the strains on the different plate conditions, *K. sucrofermentans* (monoculture replicate B from Coculture 2 after 5 days, which formed a BC pellicle) and *S. cerevisiae* IMX1812 $\rho-$ after 5 days were each plated on all three media (YPDM, YPDM + cycloheximide, YPDM + chloramphenicol) and incubated at 30 °C for three days. For the actual consortium, samples were taken from each SynCom flask at two time points: after 1.5 days of static incubation (prior to reinoculation) and at the end of the 5 day coculture. After, these samples were plated on the three media types described above and incubated at 30 °C. The plates were then compared to the monoculture controls to determine whether *S. cerevisiae* IMX1812 $\rho-$ and *K. sucrofermentans* coexisted under the coculture 2 conditions.

4 Results

4.1 Ethidium Bromide induced mitochondrial knock-out of *S. cerevisiae*

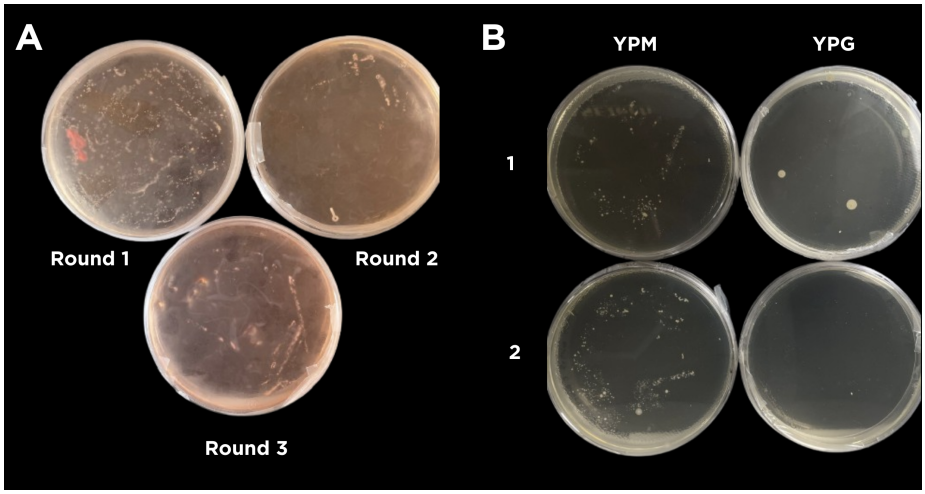

Figure 5: **Mitochondrial knock out of *S.cerevisiae* IMX1812** A. Three rounds of ethidium bromide plating of *S.cerevisiae* IMX1812. B. Replica plating *S.cerevisiae* IMX1812 on YPM (6.8 g/L maltose) and YPG (2% glycerol) with duplicates (shown as 1 and 2).

The three rounds of ethidium bromide plating were successful (Figure 5A). The gradual loss of mitochondrial function was observed through the longer

time elapsed for colonies to become visible after each round. As expected from the replica plating, the successful colonies are present on the YPM plates but absent from the YPG plates since mitochondrial function is necessary to grow on glycerol (Figure 5B). YPM liquid cultures were made from these selected colonies to proceed with investigating the growth kinetics of the newly made strain (Figure 6) to inform the preparation and interpretation of the coculture. The colonies on the YPG plate grew significantly larger, indicating that the mitochondrial function is not lost there, and more ATP can be yielded, resulting in faster growth (Figure 5B.1).

4.2 Monoculture growth kinetics

4.2.1 Growth on carbon substrates

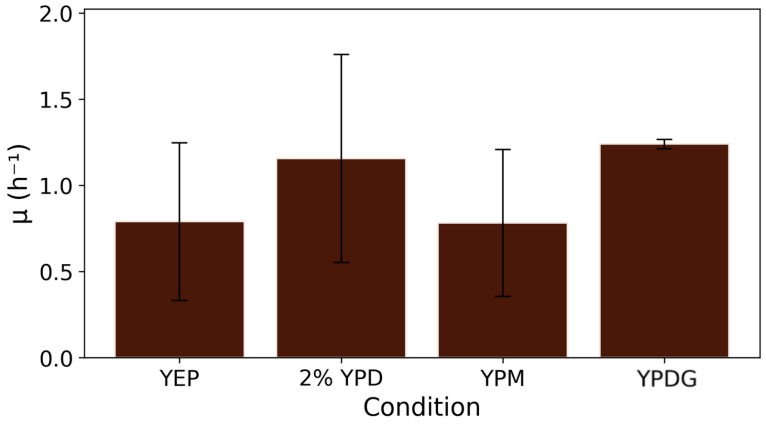

Figure 6: **Average growth rate of K.sucrofermentans on carbon substrates**. From left to right, the average growth rate per hour on yeast extract peptone (YEP) medium, 2% YPD (glucose) medium, YPM (6.8 g/L maltose), and YPDG (2% glucose and 2% glycerol) is shown. YEP is included to assess whether the addition of maltose supports growth more than the basal yeast extract and peptone medium.

The graph of *K.sucrofermentans* on the relevant carbon substrates within the coculture suggests that the presence of maltose does not lead to a higher rate of growth, with all the replicates within the same range, indicated by the error bars (Figure 6). Although not a significant difference (t ¿ 0.05), the YPDG appears to have the highest rate of growth. This condition was included since

S.cerevisiae produces glycerol in the coculture to maintain the redox balance by converting NADH back to NAD^+ (Figure 4) [24]. In literature, glycerol was shown to contribute to BC yield [2]. Due to the cellulase enzyme added to all of the *K.sucrofermentans* samples, this might have provided extra carbon for growth. Overall, the average growth rate of *K.sucrofermentans* within a monoculture can be assumed to be between 0.5-1.25μ when glucose is provided.

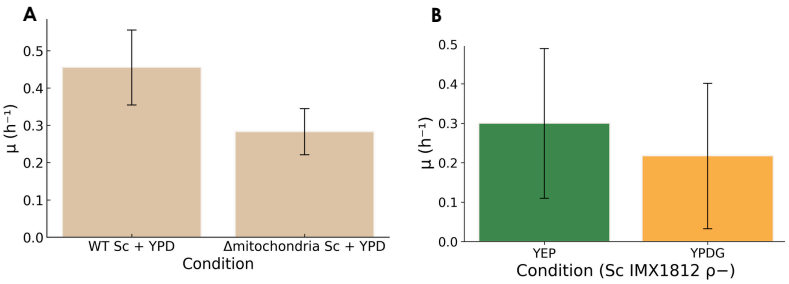

Figure 7: Average growth rate of *S.cerevisiae* A.WT vs Δ mitochondria ($\rho-$) B. IMX1812 $\rho-$ on YEP and YPDG. The YPM sample tested for *S.cerevisiae* IMX1812 $\rho-$ was not included since all replicates died after 20-48 hours, and the 2% YPD sample was not included since the lag time was up to 20 hours, suggesting contamination.

The average growth rates of WT *S.cerevisiae* vs WT *S.cerevisiae* with the loss of mitochondrial function (Figure 7A) and *S.cerevisiae* IMX1812 with the loss of mitochondrial function on YEP and YPDG (Figure 7B) is presented above. A 1.6-fold difference was observed between the average growth rates of the WT vs Δmitochondria (Figure 7A). This informed modifications to the coculturing protocol, specifically the preculturing durations, from those described for *K.rhaeuticus* and WT *S.cerevisiae* by Gilbert et al. (2021). The specific modifications are described in the methods section. It was expected that *S.cerevisiae* IMX1812 $\rho-$ would neither grow on glucose or glycerol. The growth that did occur could be due to the yeast extract and peptone present, and it should be noted that one of the replicates showed the OD reducing to the starting point after 20 hours. This is seen from the Richard's fit of the replicates (SupplementaryFigure3)

4.2.2 Growth on metabolites present during the coculture

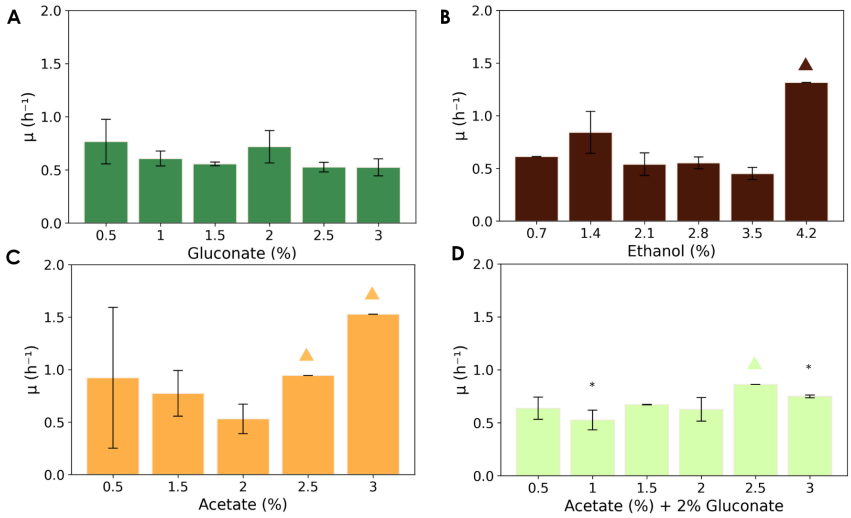

Figure 8: **Average growth rate per hour of *K.sucrofermentans* plotted against the concentration gradients of A. (sodium) gluconate, B. ethanol, C. (potassium) acetate, and D. acetate and gluconate together.** The triangles indicate that only 1 replicate is shown, and the * indicates pairs with significant differences between each other (p ¡ 0.05). 1% acetate was not included since none of the replicates had a conventional Richard's fit (Appendix7.6)

In general, the addition of the acids to *K.sucrofermentans* resulted in lower growth rates than just with YPD and YPDG (Figure 6), which was expected as the pH becomes lower (Figure 8). For the ethanol series, we can suggest that around 1.4 % (v/v) is optimal and ¿2.8 % (v/v) the growth rate depletes. In general, we can assume that the average growth rate of *K.sucrofermentans* within the coculture conditions will be between 0.5 and 1 per hour. It should be noted that the bars with triangles above them (Figure 8B,C) only show one replicate. The other replicates were removed due to unrealistically high ODs reached, and the replicates kept for these appear to still have the highest average growth rates, so no conclusions were drawn from these.

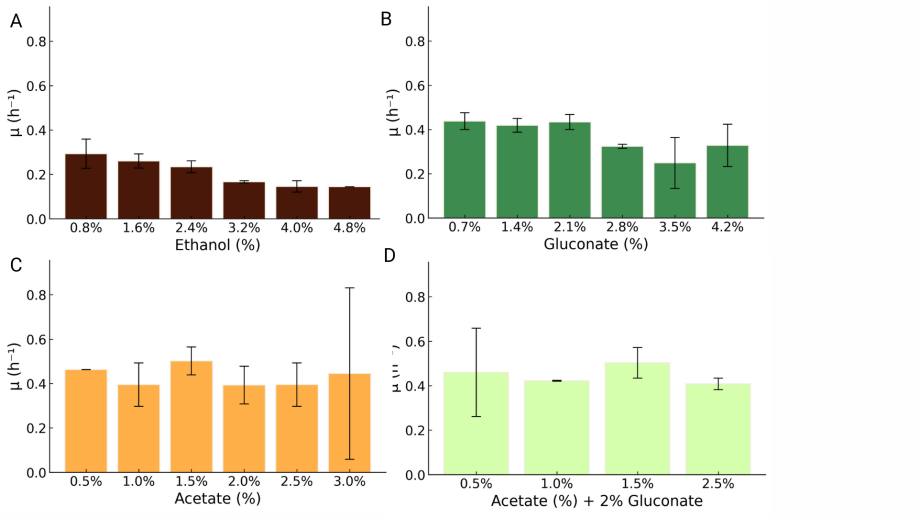

Figure 9: **Average growth rate per hour of *S.cerevisiae* CENPK113-7D $\rho-$ plotted against the concentration gradients of A. ethanol, B. (sodium) gluconate , C. (potassium) acetate, and D. acetate and gluconate together.**

Across all conditions, S. cerevisiae CENPK113-7D $\rho-$ was found to be the most sensitive towards ethanol, with even the lowest supplemented concentration of ethanol having a smaller growth rate than the average of the growth rate's observed for other conditions (Figure 9). For this concentration range, the results suggest that there there is a trend where growth rate decreases with increasing ethanol (Figure 9A). Growth is generally maintained amongst the acetate concentrations (excluding the 3.0% acetate condition where the error bar is very large), showing that this strain has a tolerance towards acetate (up to 2.5% (w/v)) (Figure 9C). The gluconate conditions show a similar tolerance, and the μ starts to decrease beyond 2.1% gluconate, notably a similar amount of acid leading to the μ decreasing in acetate too (Figure 9B). The combined acid condition also shows similar growth rates as in just acetate and just gluconate (Figure 9D). The gluconate, acetate, and combined acid conditions show that the μ reached here are comparable, if not higher, to those reached in just YPD for this strain (Figure 7A) (See Discussion 4.1). Largely, the average growth rate of the strain *S.cerevisiae* CENPK113-7D $\rho-$ can be said to be slightly lower than that of *K.sucrofermentans*.

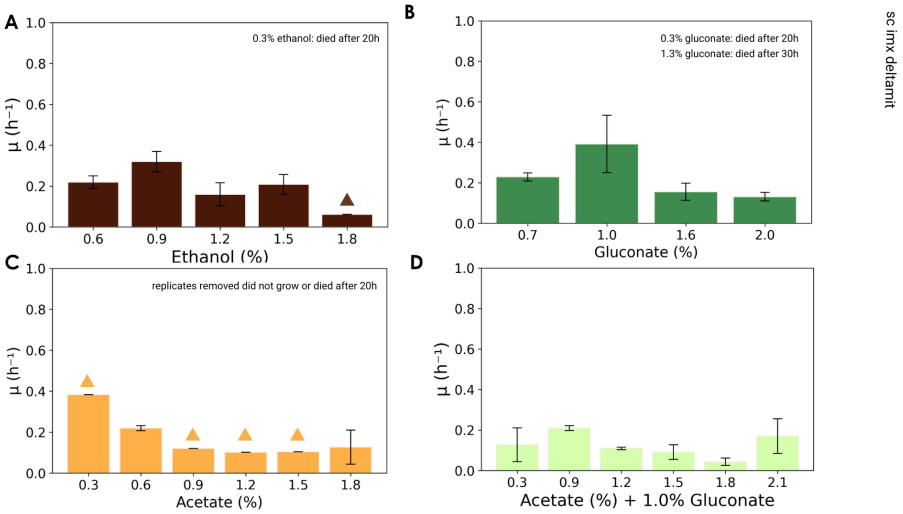

Figure 10: **Average growth rate per hour of *S.cerevisiae* IMX1812 $\rho-$ plotted against the concentration gradients of A. ethanol, B. (sodium) gluconate , C. (potassium) acetate, and D. acetate and gluconate together.**

There is a directly observable reduction in the growth rate for the strain *S. cerevisiae* IMX1812 $\rho-$. The highest growth rates for this strain are observed for the 0.9% ethanol, 1% gluconate, and 0.3% acetate (noting that only one replicate survived 3 days) samples. The combined acid samples, except for 0.9% acetate + 1% gluconate and 2.1% acetate + 1% gluconate, notably have even lower growth rates. Overall, it appears that the strain *S.cerevisiae* IMX1812 $\rho-$ is not sufficiently robust and is experiencing a metabolic burden upon the mitochondrial knock out that is making it grow significantly slower and not consistently survive for over 20-30 hours.

4.3 Coculture 1: S.cerevisiae IMX1812 and *K.sucrofermentans*

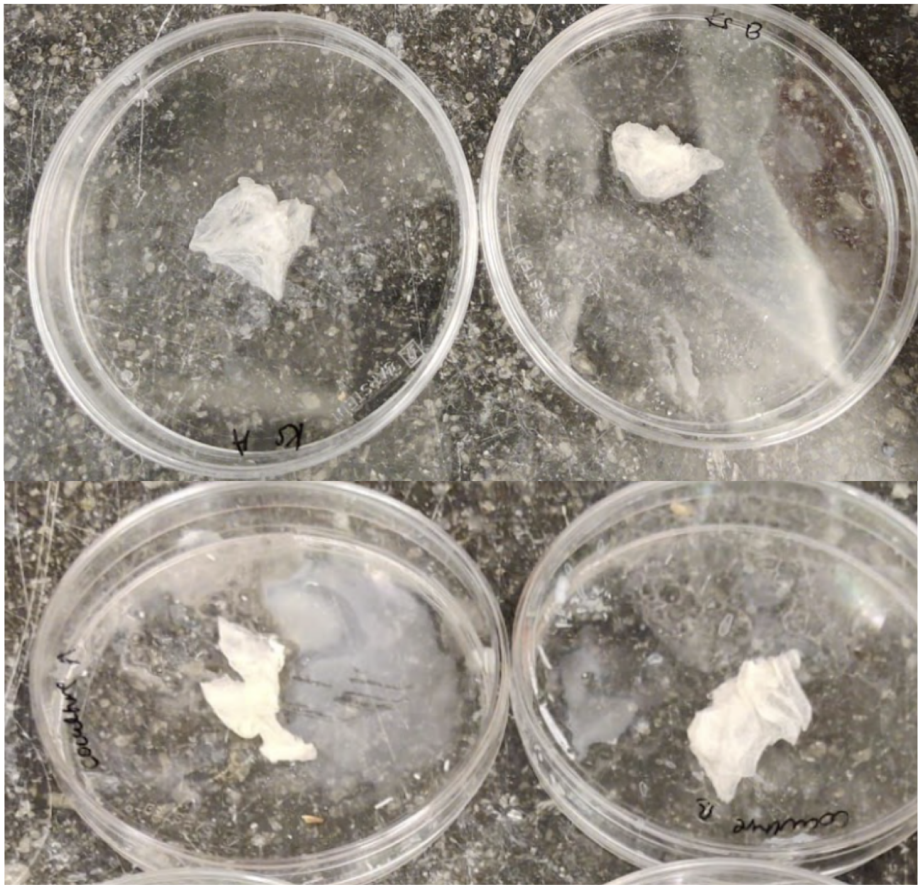

Figure 11: **The cellulose pellets formed in the *K.sucrofermentans* monoculture vs. the coculture between *S.cerevisiae* and *K.sucrofermentans*.** Top two plates contain the pellets from the monoculture duplicates while the bottom two plates contain the pellets from the coculture duplicates

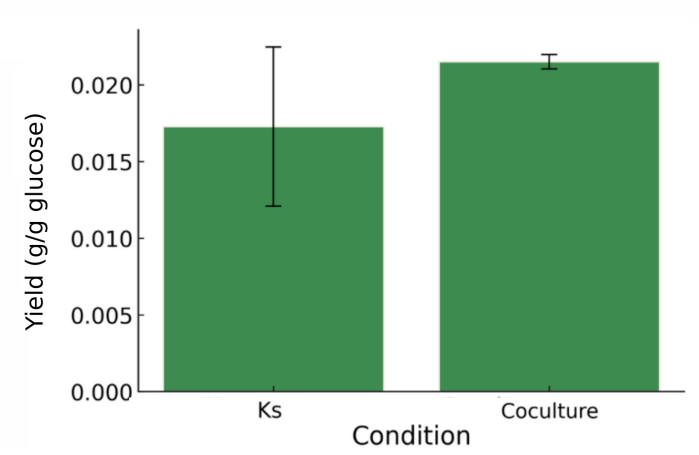

Figure 12: **Comparing the BC yields from the monoculture vs coculture** The yield was calculated in terms of grams of BC per grams of glucose provided in the medium at the start of cultivation.

The cellulose pellicles from the duplicate *K.sucrofermentans* monocultures and duplicate cocultures looked approximately the same to the naked eye after freeze-drying (Figure 11). This was confirmed by the calculated yields (g BC/g glucose fed) (Figure 12). The hypothesis was that the BC yielded from the coculture would be comparable or higher, which was achieved.

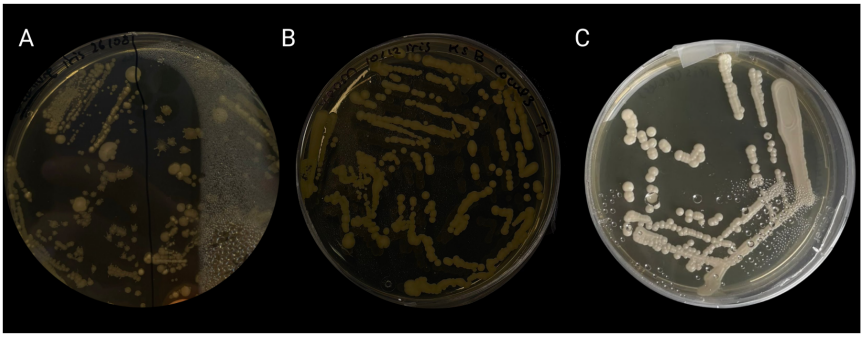

Figure 13: **Assessing coexistence in coculture 1** A. The pellets obtained from centrifuging the duplicate coculture samples were plated on a YPDM plate, with both duplicates shown on one half of the plate. B. The phenotype of *K.sucrofermentans* on a YPD plate as reference. C. The phenotype of *S.cerevisiae* IMX1812 on a YPM plate

Comparing the phenotype of the distinct two strains on both halves YPDM plate with the phenotype of the strains, it appears that, after four days, both species survived (Figure 12A). This is assumed since the smaller, whiter, convex and round colonies appear to be the same species as in Figure 12C, while the colonies with a yellow undertone, irregular shape, and that are flatter looks like the *K.sucrofermentans* colonies in Figure 12B. The colonies hypothesised to be *S.cerevisiae* IMX1812 look smaller in the coculture plate (Figure 12A) than that of its monoculture plate (Figure 12C), which might be due to less growing time allowed.

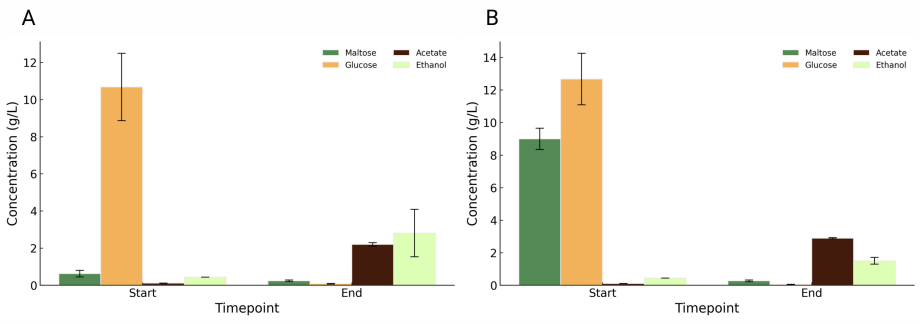

Figure 14: **HPLC analysis of the start and endpoint samples of *K.sucrofermentans* monoculture and coculture 1** A. *K.sucrofermentans* B. Coculture 1. Only start and end results were shown as there was no clear difference between the compositions of the samples taken during the first day. Dark green = maltose, orange = glucose, brown = acetate, light green = ethanol

The results of the HPLC analysis show that glucose was consumed and acetate was produced in both monoculture (Figure 14A) and co-culture (Figure 14B). As only start and endpoint samples were taken, we cannot determine if *K.sucrofermentans* is consuming the ethanol produced by *S. cerevisiae*. However, ethanol was produced in the medium. The small amount of maltose at the start of the monoculture is likely carryover, since maltose was not added to this medium.

Ethanol production in the monoculture samples was not expected. Two hypotheses may account for this observation. The first one is that there is a metabolic pathway in *K. sucrofermentans* able to produce ethanol, that we are not aware of. The second one is that the supernatant of the monoculture sample had a small amount of *S. cerevisiae* cells remaining, that consumed the carry over maltose and produced ethanol. To test this hypothesis, a colleague modeled this small amount of contamination and the levels of acetate and ethanol that would be the outcome of this. The model supported that this would yield more ethanol than acetate, suggesting that this hypothesis might be likely [30] .

4.4 Coculture 2:*S.cerevisiae* IMX1812 $\rho-$ and *K.sucrofermentans*

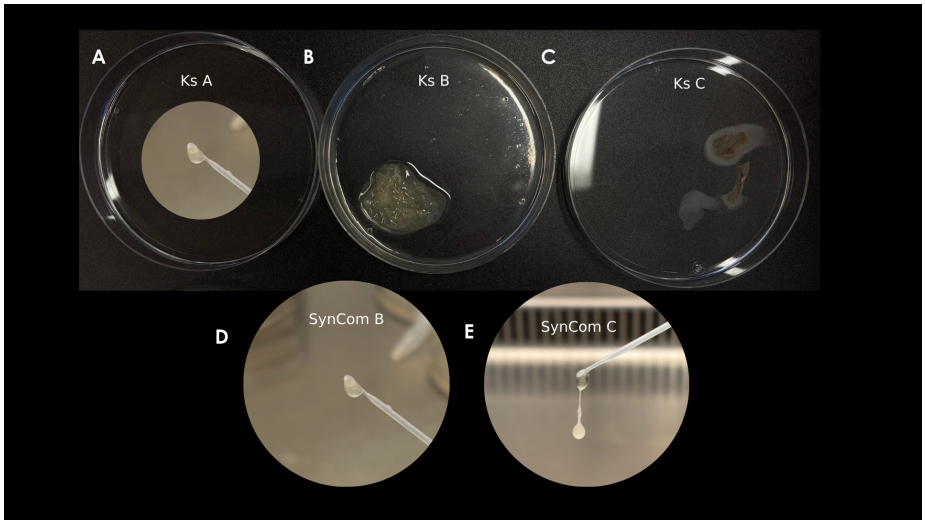

Figure 15: **The total bacterial cellulose outcome from the second coculture experiment** A. Shows replicate A of *K.sucrofermentans* monoculture control, with no BC production but an exopolysaccharide in the sample taken for plating (Figure 15). B. shows replicate B of *K.sucrofermentans* monoculture control, with a BC pellet without downstream processing or freeze drying. C. shows very small BC or exopolysaccharide formation. D and E show small pieces of slime-like exopolysaccharide noticed during plating, since none of the SynCom replicates showed an observable BC pellet or pellicles that could be separated

The total BC obtained in the second coculture experiment (coculture 2) was not as expected (Figure 15). Under static conditions, none of the SynCom triplicates formed an observable BC pellicle. However, small, slimy polymer fragments were observed in samples taken for plating to assess coexistence. In the *K. sucrofermentans* monoculture controls, triplicate B produced a clear BC pellet at the air–liquid interface, whereas triplicate A did not form a pellicle but contained the same slimy polymer in the sample taken for plating (Figure 15). Triplicate C showed only very small BC or polymer aggregates that could not be harvested as one single pellet. Overall, BC formation in coculture 2 was absent in all SynCom replicates and unstable in the *K. sucrofermentans* monoculture.

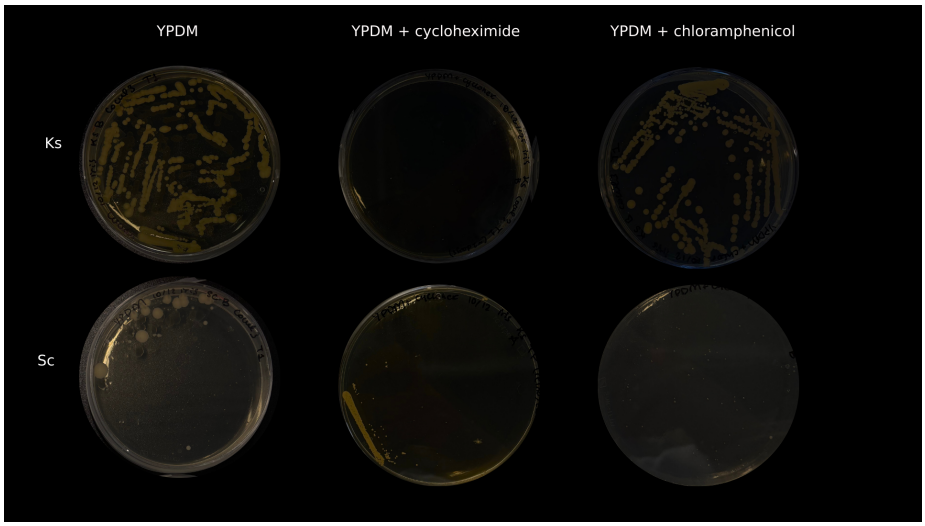

Figure 16: **Controls for assessing the coexistence in coculture 2** Ks: *K. sucrofermentans* (Duplicate B from the experiment that did from the BC pellicle), and Sc: *S.cerevisiae* IMX1812 $\rho-$ plated on YPDM, YPDM + 150 microliter cycloheximide to select for *S.cerevisiae*, and YPDM + 185μg/mL chloramphenicol to select for *K.sucrofermentans* containing the antibiotic marker.

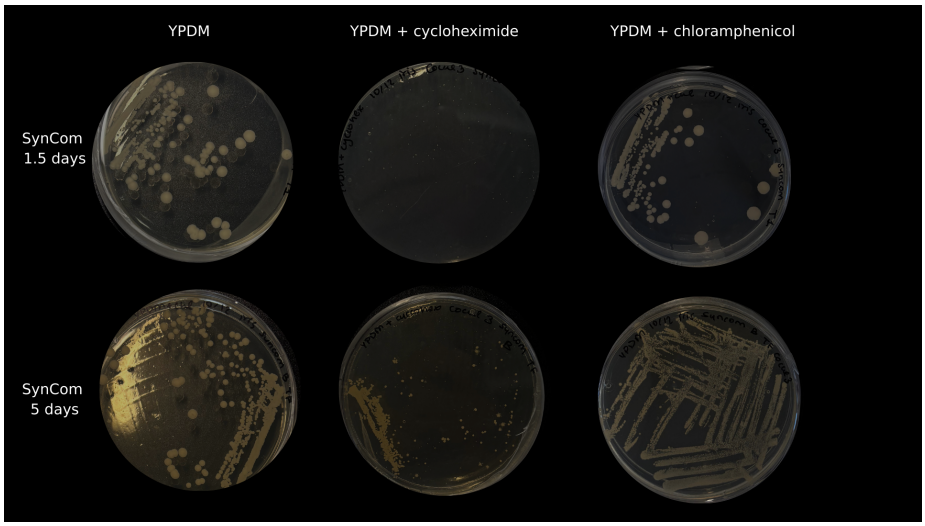

Figure 17: **Assessing the coexistence in coculture 2.** 1.5 days and 5 days after cultivation SynCom B (Triplicate B of *S.cerevisiae* IMX1812 $\rho-$ and *K.sucrofermentans* Final plated on YPDM, YPDM + 150 microliter cycloheximide to select for *S.cerevisiae*, and YPDM + 185μg/mL chloramphenicol to select for *K.sucrofermentans* containing the antibiotic marker. Upon the observation that there is no BC production, all SynCom and *S* triplicates

K. sucrofermentans (monoculture triplicate B, which had formed a pellicle) and S. cerevisiae IMX1812 $\rho-$ were plated as controls on YPDM, YPDM + cycloheximide, and YPDM + chloramphenicol (Figure 16). As expected, the *K. sucrofermentans* control grew on both YPDM and chloramphenicol plates, confirming chloramphenicol resistance, while the *S. cerevisiae* control formed visibly smaller colonies on cycloheximide plates than on YPDM and showed almost no growth on chloramphenicol, aside from a single small colony on the lower right of the plate. This suggests that another selection method should be chosen in the future for *S.cerevisiae*.

Coexistence in coculture 2 was then assessed by plating samples from SynCom triplicate B at two time points on the same three media types (Figure 17). The culture sampled after 1.5 days of static incubation (before reinoculation) yielded colonies on YPDM and chloramphenicol plates, while cycloheximide plates showed either very small colonies or no clear growth, but due to the presence of bubbles the yeast detection at this first time point is inconclusive. In contrast, the culture sampled after 5 days (following reinoculation at 1.5 days) produced colonies on all three plate types. The presence of colonies on both cycloheximide and chloramphenicol plates indicates that although the control *S. cerevisiae* IMX1812 $\rho-$ is not reliable, the *K.sucrofermentans* strain showed no growth at all on cycloheximide on the control sample. It can be concluded

that *K. sucrofermentans* survived in coculture 2 for at least 5 days, despite the lack of detectable BC pellicle formation in the SynCom conditions. However, the possibility that there is also contamination present in these samples should be considered.

5 Discussion

5.1 Monoculture growth kinetics of *K.sucrofermentans* and engineered *S.cerevisiae*

The monoculture growth kinetics experiments provided information about the relative rate of growth of the coculture partners in the presence of organic acids and ethanol that we expect to be present during the coculture. The experiments showed that *K. sucrofermentans* grew consistently on YPD media while the induced knock-out of the mitochondria (ρ^- strains) reduced the growth rate of both WT *S. cerevisiae* CEN.PK, and IMX1812 ρ^-. Moreover, IMX1812 ρ^- was no longer able to consistently grow during three-day microplate reader assays.

In the gluconate, acetate, ethanol, and gluconate and acetate gradient assays, *K. sucrofermentans* growth was supported up to intermediate concentrations. For the yeast strains, acetate and gluconate on YPD had relatively modest effects on CEN.PK ρ^-, whereas IMX1812 ρ^- was substantially more sensitive, particularly under the combined acid conditions. Therefore, *K. sucrofermentans* and *S.cerevisiae* IMX1812 have a reasonably larger margin of stability with respect to coculture medium composition compared to IMX1812 ρ^-, which has weakened growth to begin with.

Comparison of WT $\rho-$ yeast grown in YPD (Figure 7A) with and without added ethanol or acids (Figure 9) demonstrates that, overall, the addition of acids to the YPD medium either supported or did not affect growth. Biologically, this makes sense as *Saccharomyces* sp. often naturally exists with acetic acid bacteria in slightly acidic pH, where they ferment sugars to ethanol and AAB oxidises ethanol to acetate. Examples include the previously mentioned kombucha cultures, but also vinegar ecosystems and fruit rotting. The yeast being fermentative also mimics these environments in which the yeast is in reduced oxygen while the AAB accumulates in the oxygen-rich interfaces as an obligate aerobe. This is not the case for the addition of ethanol concentrations over 1.6% (v/v). Theoretically, fermentative *S.cerevisiae* can maximally produce around 0.51 g ethanol/g glucose. For the coculture this means: $\tilde{1}$.3% (v/v ethanol). The theoretical yield of acetate and gluconate in the coculture would be 1.33% and 0.8%, which, when looked at Figure 8C (1.0-1.5% for acetate and 0.7-1.4% for gluconate) seemingly boosts growth compared to just the YPD medium.

5.1.1 Dissociation of the organic acids depends on the pH of the culture

An important factor to consider is that the metabolite gradients were performed with sodium gluconate and potassium acetate salts at near neutral starting pH. In coculture 1, the endpoint pH dropped to approximately 4 (See Appendix7.7), which strongly changes the speciation of the organic acids. Acetic acid has a pK_a of approximately 4.75. at pH 4, 85.19% of the total acetate is expected to be present as undissociated acetic acid, which will enter the cell and become more inhibitory than acetate anions. Gluconic acid has a pK_a in the range of 3.6 to 3.8, so, at pH 4, 30.4% of the total gluconate pool is predicted to be in the undissociated form. This theoretical speciation can be combined with yield calculations to estimate a upper bound of possible acid stress in the coculture. If all of the glucose (20 g/L) provided were converted to acetate (glucose $\rightarrow$ 2 acetyl-CoA $\rightarrow$ 2 acetate), the maximum yield would be about 0.67 grams of acetate per gram glucose, corresponding to 1.33% w/v acetate (calculations in Appendix7.8). Similarly, assuming the reported yield [8] of 0.39 grams gluconate per grams of glucose, full conversion of glucose would yield 0.78% (w/v) gluconate. At pH 4, this theoretical maximum translates to roughly 1.1% undissociated acetic acid and 0.3% undissociated gluconic acid. It is known that full conversion can not happen, since BC production is observed. Metabolically, *Komagataeibacter* produces acetate by oxidising ethanol (ethanol $\rightarrow$ acetaldehyde via alcohol dehydrogenase; acetaldehyde $\rightarrow$ acetate via aldehyde dehydrogenase in the periplasm) and by converting acetyl-CoA formed from glucose catabolism via phosphotransacetylase or acetate kinase. In the presence of yeast, the first route couples directly to the ethanol derived from the yeast, while the second route can produce acetate in the absence of yeast too. These considerations suggest that both the presence of yeast and intrinsic *Komagataeibacter* metabolism may contribute to acid accumulation in the coculture as the pH drops.

5.2 Coexistence and BC production in Coculture 1

Coculture 1 showed successful BC production and coexistence occured. However, the stability of this coexistence can be questioned. A static SynCom of *K. sucrofermentans* and *S. cerevisiae* IMX1812 produced BC yields comparable to, or even slightly higher than the monoculture (Figure 12). Although the cultivation flask, sampling set-up and the harvesting method had shortcomings and should be improved, the pellicles in the coculture (Figure 11) were similar in appearance and texture to those of the monoculture. Plating suggested that both partners were present at the end of the four day coculture judging by the phenotypes observed (Figure 13), so coexistence is feasible. HPLC analysis (Figure 14) showed glucose and maltose consumption in the coculture. Moreover, there is a very small reduction of maltose in the monoculture where maltose was not expected at the start at all. As expected, there is acetate accumulation

in both the monoculture and coculture. However, the detection of ethanol in the monoculture raises questions. Puvvada (2025) modelled a small amount of of *S.cerevisiae* contamination with the maltose observed at the start of the monoculture ($\tilde{0}$.62 g/L). The simulation qualitatively matched the HPLC data obtained [30]. However, it is seen that the maltose is not even completely consumed ($\tilde{0}$.24 g/L) in the monoculture (Appendix7.5.2, Table 3) Theoretically,

$$1\ \text{glucose} \ \rightarrow\ 2\,\text{ethanol} + 2\,\text{CO}_2 \tag{1}$$

$$1\ \text{maltose} \ \rightarrow\ 2\,\text{glucose} \ \rightarrow\ 4\,\text{ethanol} + 4\,\text{CO}_2 \tag{2}$$

. This amount of maltose consumed theoretically corresponds to 4 x (0.62-0.24) = 1.52 g/L ethanol. The ethanol that is produced at the end is $\tilde{2}.8\pm1.28$, so the theoretical amount of ethanol is very similar to the lower bound of the error range. However, since the maximum theoretical yield is not likely to be reached, this hypothesis is not very probable. Since the sampling frequency was limited, ethanol consumption by *K. sucrofermentans* cannot be conclusively demonstrated. Nonetheless, the combination of ethanol production by yeast, acetate accumulation and sustained BC formation suggests that the intended exchange of metabolites is at least partially working: *K. sucrofermentans* focuses on BC production from glucose, while yeast uses maltose and supplies ethanol that can be oxidised by the bacterium to boost the energy metabolism (as in Figure 1, Figure 4). This interpretation is consistent with previous reports that low to moderate ethanol supplementation can support BC production by *Komagataeibacter* species [22].

5.3 Loss of BC in Coculture 2 the possibility of Cel$^-$ emergence

Coculture 2 revealed a clear bottleneck. When the maltose-consuming *S. cerevisiae* IMX1812 was replaced with the fermentative (ρ^-) IMX1812 strain, even upon reducing the starting OD of *Komagataeibacter* and extending the preculture time for the yeast, the effects of acid accumulation or agitation stress were still observed. It can still be argued that coexistence did occur, selective plating of the SynCom showed colonies on both cycloheximide and chloramphenicol plates while colonies known to be *K.sucrofermentans* died in the presence of cycloheximide. However, none of the SynCom replicates formed a coherent BC pellicle, and the *S.cerevisiae* control plate did not behave as expected. Instead of the pellicle, small, slime-like polymer fragments were observed. Even the *K. sucrofermentans* monoculture behaved inconsistently, with only one of three replicates forming a pellicle expected from stable static cultivation. A contaminant is causing these unexpected results is also possible.

In literature, it is discussed that prolonged agitation or medium composition of *Komagataeibacter* cultures can make another process bottleneck appear, which might explain the loss of pellicle formation in the second coculture. *Ko-*

magataeibacter can have spontaneous appearance of cellulose-negative (Cel^-) mutants within *Komagataeibacter* populations. Since Cel^- mutants do not have the metabolic burden of cellulose synthesis, this can confer a growth advantage over Cel^+ cells, leading to a decline in cellulose yield, and Cel^+ phenotypes within the culture. [29, 29, 42, 36]. Park et al. (2004) showed that the addition of organic acids such as glutamic and acetic acid promoted the conversion of Cel^+ cells into Cel^- mutants in shaken flask cultures. Adding 1% (v/v) ethanol to these media either reduced or increased Cel^- formation according to flask geometry and the attributed shear stress. Moreover, Taweecheep et al. (2019) identified a nonsense mutation in the *bcsC* gene (one of the 4 genes in the BC synthase operon) in an ethanol adapted strain of *Komagataeibacter oboediens* that no longer showed BC production. Upon repeated recultivations in static conditions, they obtained revertant strains that revived their ability to produce BC, however exhibiting different productivities and fibrillar structures. Thus, point mutations in genes as a result of the presence of medium stress, and agitation conditions, can both eradicate and restore BC synthesis, causing changes to morphology of the material [36]. Considering these findings, under the conditions of coculture 2, with 1) potentially more ethanol available for *K.sucrofermentans* to convert to acetate through the prevention of reassimilation by yeast, and 2) less fresh preculture inocula of that have been agitated before, a point mutation might have been induced in one of the genes in the *bcs* operon. The fermentative yeast, although not consuming ethanol, is also expected to have produced less ethanol overall because of its slowed growth kinetics. On the other hand, additional to the oxidation of ethanol in the periplasm, the glucose metabolism by *K. sucrofermentans* itself can produce acetate via acetyl-CoA. Several studies had reported Cel^- mutants emerged in the presence of high acetic acid, and high ethanol concentration combined with shear and shaking [29, 28, 36]. These explanations remain hypotheses because the potential Cel^+ and Cel^- populations from coculture 2 were not isolated and sequenced. However, they are qualitatively consistent with BC synthesis loss. A logical next step would be to sequence the *bcs* operon and key regulatory genes in endpoint *K. sucrofermentans* isolates to confirm this.

5.4 BC coculture strategy with *Komagataeibacter* and *S.cerevisiae*: expected challenges and future prospects

Coculture 1 demonstrated that a *K. sucrofermentans* and *S. cerevisiae* consortium can coexist and produce BC while keeping glucose and maltose largely segregated between partners. This conceptually highlights a potential Syn-SCOBY system that aims to use yeast to functionalise BC produced by *Komagataeibacter* sp. In contrast, Coculture 2 illustrates how sensitive such systems can be to strain robustness, acid stress, and trade-offs with agitation (Figure 18A). Changes in the yeast chassis and preculture conditions may have pushed the system into a Cel^- dominated regime where BC production is no longer stable.

Several limitations of the present work can be listed. All coculture experiments were carried out in Erlenmeyer flasks, where subtle differences in handling can have large effects. BC characterisation was limited to approximate productivity and we did not check changes to the fibrillar structure. Our inference about Cel^+ vs. Cel^- composition is indirect, based on process outcomes and literature, and not backed by conclusive methods. Finally, the full potential of the yeast partner for active functionalisation was not yet exploited for example through the in-situ secretion of enzymes or display of functional proteins or dyes on the BC matrix (Figure 18B1).

Despite the limitations, this study describes and further reveals the main challenges and prospects of BC production in a synergistic coculture between *Komagataeibacter* and *S. cerevisiae* (Figure 18). In future designs, not only the presence of ethanol but also its production dynamics will need to be tuned. In particular, there is likely to be an optimal balance between the rate at which yeast produces ethanol (which supports BC formation) and the total amount that accumulates (which drives acetate build-up and pH toxicity). Such a balance could, in principle, be achieved by engineering regulatory circuits in *S.cerevisiae* that modulate ethanol production in response to internal or extracellular signals (e.g. intracellular ethanol concentration, pH or BC formation) thereby keeping ethanol within a beneficial range. Alternatively, controlling the substrate supply of maltose through fed-batch or continuous feeding strategies could be used to limit total ethanol formation, although this will be more challenging when using heterogeneous waste-derived substrates. Additionally, creating a yeast that will alleviate process bottlenecks while supporting its own growth might enhance stability. This could be done through the redox engineering of *S.cerevisiae* as described by Medina et al.. In this approach, yeast is engineered to consume acetate as an electron acceptor to reduce glycerol formation. This can be achieved with the deletion of two genes (glycerol-3-phosphate dehydrogenases) and heterologous expression of the*mhpF* gene from *E.coli* [19]. The yeast could also be engineered to consume the gluconic acid in the medium for growth through expressing a heterologous gene for the transport of gluconic acid, although this has not been reported to date. This approach would enable establishing a cross-feeding mechanism where the yeast consumes acetate/gluconate produced by *Komagataeibacter* and provides ethanol in return. This cycling between the coculture members could allow for a tighter dependency between the coculture partners. Moreover, this could inform how to control the ethanol concentration in the system through the optimization of inoculum ratios and substrate composition. As next steps, when moving to controlled bioreactors, reactor design and operating strategy would have to balance three coupled objectives: maintaining sufficient oxygen transfer, avoiding stress regimes that favour Cel^- selection, and preserving a BC morphology that can be harvested and processed efficiently. In parallel, systems biology tools could be used to formalise and explore these trade-offs. A logical starting point would be dynamic, ODE-based models that describe the time evolution of the key state variables in the coculture, namely, the biomass of each partner, metabolite con-

centrations and BC. Such models could be parameterised with the monoculture kinetics and coculture data obtained in this work and then used to simulate how, for instance, different genome engineering methods for an ethanol circuit can affect BC yield and acid accumulation.

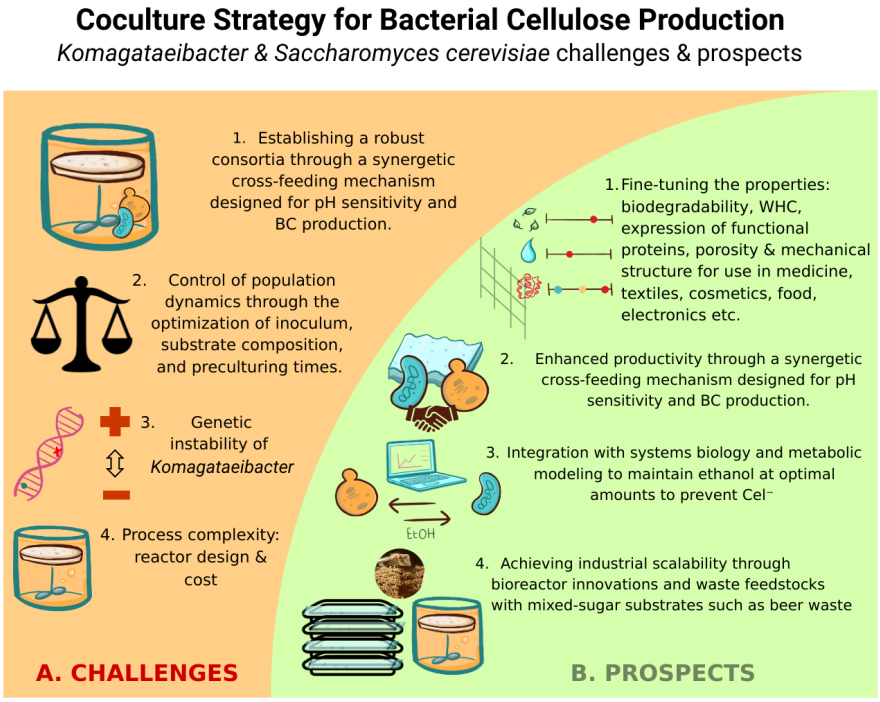

Figure 18: **Summary of challenges and future prospects for the coculture approach to BC production with *Komagataeibacter* and *Saccharomyces cerevisiae*** Figure inspired by Absharina et al. challenges and prospects of coculture approach to BC production (2025) [1].

6 Conclusion

This study set out to test a coculture design for robust BC production between the model SynBio organism *Saccharomyces cerevisiae* and a model BC-producing organism, *Komagataeibacter sucrofermentans*. These strains were selected because *S. cerevisiae* could potentially overcome key bottlenecks in BC production by (i) providing ethanol, which is beneficial for BC synthesis at concentrations up to 1.5%, (ii) tolerating accumulation of acetic acid or gluconic acid, (iii) the naturally occurring synergistic behaviour in SCOBY cultures ,

and (iv) the ability to consume waste derived substrates. In addition, a fermentative yeast was obtained to ensure the ethanol is not consumed by itself. The greater advantage of including the model SynBio organism *S.cerevisiae* is enabling functionalising and fine tuning BC for various applications. The system was designed to prevent competition for the carbon substrates used for growth and BC production by constraining yeast to maltose as carbohydrate and energy source, while glucose was primarily directed towards cellulose synthesis, and yeast-produced ethanol could support *Komagataeibacter* energy metabolism. To test this hypothesised system, three main questions were asked: whether coexistence could be achieved and if coculturing i) maintains the BC yield, and ii) mitigates the drawbacks in the process caused by acid accumulation. Respectively, it was found that *K. sucrofermentans* and *S. cerevisiae* IMX1812 can coexist while maintaining BC yields, but that the drawbacks should be mitigated with tighter control of the process. Looking ahead, combining systems biology, strain engineering to manage acid accumulation and tolerance, bioreactor optimisation to control oxygen and shear, and explicit monitoring of robustness under perturbations will be essential for industrial production of functionalised bacterial cellulose. Overall, this work represents a stepping stone towards a model Syn-SCOBY platform rather than a finished system.

Artificial Intelligence Usage
No artificial intelligence (AI) was used in the writing of this thesis. Large language AI models, namely GPT-5.1, was used to convert an R script to Python, LaTeX scripts (especially for the Appendix), brainstorming the structure of the introduction, and to check grammar when finalising the thesis.

References

[1] Dheanda Absharina et al. "Bacterial Cellulose Production in Co-Culture Systems: Opportunities, Challenges, and Future Directions". en. In: *Applied Microbiology* 5.3 (Sept. 2025). Publisher: Multidisciplinary Digital Publishing Institute, p. 92. ISSN: 2673-8007. DOI: 10.3390/applmicrobiol5030092. URL: https://www.mdpi.com/2673-8007/5/3/92 (visited on 12/04/2025).

[2] A. Adnan et al. "Glycerol as a cheaper carbon source in bacterial cellulose (BC) production by *Gluconacetobacter xylinus* DSM46604 in batch fermentation system". In: *Malaysian Journal of Analytical Sciences* 19.5 (2015), pp. 1131–1136.

[3] *Bioeconomy & European Green Deal — Knowledge for policy.* URL: https://knowledge4policy.ec.europa.eu/bioeconomy/bioeconomy-european-green-deal_en (visited on 12/04/2025).

[4] Pedro R. Brandão, Maria T. B. Crespo, and Francisco X. Nascimento. "Phylogenomic and comparative analyses support the reclassification of several Komagataeibacter species as novel members of the Novacetimonas gen. nov. and bring new insights into the evolution of cellulose synthase genes". en. In: *International Journal of Systematic and Evolutionary Microbiology* 72.2 (Feb. 2022). ISSN: 1466-5026, 1466-5034. DOI: 10.1099/ijsem.0.005252. URL: https://www.microbiologyresearch.org/content/journal/ijsem/10.1099/ijsem.0.005252 (visited on 12/04/2025).

[5] P. Deshpande et al. "Bacterial cellulose: Natural biomaterial for medical and environmental applications". In: *Journal of Natural Fibers* 20.2 (2023). DOI: 10.1080/15440478.2023.2218623. URL: https://doi.org/10.1080/15440478.2023.2218623.

[6] "Effect of ethanol on bacterial cellulose production from fructose in continuous culture". en-US. In: *Journal of Fermentation and Bioengineering* 85.6 (Jan. 1998). Publisher: Elsevier, pp. 598–603. ISSN: 0922-338X. DOI: 10.1016/S0922-338X(98)80012-3. URL: https://www.sciencedirect.com/science/article/pii/S0922338X98800123 (visited on 04/14/2025).

[7] *Engineering control of bacterial cellulose production using a genetic toolkit and a new cellulose-producing strain.* en. DOI: 10.1073/pnas.1522985113. URL: https://www.pnas.org/doi/10.1073/pnas.1522985113 (visited on 12/01/2025).

[8] *Engineering PTS-based glucose metabolism for efficient biosynthesis of bacterial cellulose by Komagataeibacter xylinus - ScienceDirect*. URL: https://www.sciencedirect.com/science/article/pii/S0144861724006854 (visited on 11/19/2025).

[9] Meirong Gao, Deon Ploessl, and Zengyi Shao. "Enhancing the Co-utilization of Biomass-Derived Mixed Sugars by Yeasts". English. In: *Frontiers in Microbiology* 9 (Jan. 2019). Publisher: Frontiers. ISSN: 1664-302X. DOI: 10.3389/fmicb.2018.03264. URL: https://www.frontiersin.orghttps://www.frontiersin.org/journals/microbiology/articles/10.3389/fmicb.2018.03264/full (visited on 04/18/2025).

[10] Hamada El-Gendi et al. "Recent advances in bacterial cellulose: A low-cost effective production media, optimization strategies and applications". In: *Cellulose* 29.14 (2022), pp. 7495–7533. DOI: 10.1007/s10570-022-04697-1. URL: https://doi.org/10.1007/s10570-022-04697-1.

[11] Charlie Gilbert et al. *Living materials with programmable functionalities grown from engineered microbial co-cultures*. en. Pages: 2019.12.20.882472 Section: New Results. Dec. 2019. DOI: 10.1038/s41563-020-00857-5. URL: https://www.biorxiv.org/content/10.1101/2019.12.20.882472v1 (visited on 12/09/2025).

[12] Vivianne J. Goosens et al. "*Komagataeibacter* Tool Kit (KTK): A Modular Cloning System for Multigene Constructs and Programmed Protein Secretion from Cellulose Producing Bacteria". en. In: *ACS Synthetic Biology* 10.12 (Dec. 2021), pp. 3422–3434. ISSN: 2161-5063, 2161-5063. DOI: 10.1021/acssynbio.1c00358. URL: https://pubs.acs.org/doi/10.1021/acssynbio.1c00358 (visited on 12/04/2025).

[13] Nathan I. Johns et al. "Principles for Designing Synthetic Microbial Communities". In: *Current opinion in microbiology* 31 (June 2016), pp. 146–153. ISSN: 1369-5274. DOI: 10.1016/j.mib.2016.03.010. URL: https://pmc.ncbi.nlm.nih.gov/articles/PMC4899134/ (visited on 12/10/2025).

[14] Jared Kehe et al. "Positive interactions are common among culturable bacteria". In: *Science Advances* 7.45 (2021), eabi7159. DOI: 10.1126/sciadv.abi7159. eprint: https://www.science.org/doi/pdf/10.1126/sciadv.abi7159. URL: https://www.science.org/doi/abs/10.1126/sciadv.abi7159.

[15] A Krystynowicz et al. "Factors affecting the yield and properties of bacterial cellulose". en. In: *Journal of Industrial Microbiology and Biotechnology* 29.4 (Oct. 2002), pp. 189–195. ISSN: 1367-5435, 1476-5535. DOI: 10.1038/sj.jim.7000303. URL: https://academic.oup.com/jimb/article/29/4/189-195/5989275 (visited on 12/04/2025).

[16] Jérôme Lefebvre, Benoit Genestie, and Alexandre Leblanc. "Cellulose-Based Acoustic Absorber with Macro-Controlled Properties". en. In: *Acoustics* 6.4 (Dec. 2024). Publisher: Multidisciplinary Digital Publishing Institute, pp. 1088–1099. ISSN: 2624-599X. DOI: 10.3390/acoustics6040059. URL: https://www.mdpi.com/2624-599X/6/4/59 (visited on 12/04/2025).

[17] Guohui Li et al. “Research progress of the biosynthetic strains and pathways of bacterial cellulose”. en. In: *Journal of Industrial Microbiology and Biotechnology* 49.1 (Jan. 2022), kuab071. ISSN: 1367-5435, 1476-5535. DOI: 10.1093/jimb/kuab071. URL: https://academic.oup.com/jimb/article/doi/10.1093/jimb/kuab071/6373448 (visited on 12/04/2025).

[18] Koray Malcı et al. “Modulating Microbial Materials - Engineering Bacterial Cellulose with Synthetic Biology”. en. In: *ACS Synthetic Biology* 13.12 (Dec. 2024), pp. 3857–3875. ISSN: 2161-5063, 2161-5063. DOI: 10.1021/acssynbio.4c00615. URL: https://pubs.acs.org/doi/10.1021/acssynbio.4c00615 (visited on 10/01/2025).

[19] Víctor Guadalupe Medina et al. “Elimination of Glycerol Production in Anaerobic Cultures of a Saccharomyces cerevisiae Strain Engineered To Use Acetic Acid as an Electron Acceptor”. In: *Applied and Environmental Microbiology* 76.1 (Jan. 2010). Publisher: American Society for Microbiology, pp. 190–195. DOI: 10.1128/AEM.01772-09. URL: https://journals.asm.org/doi/10.1128/aem.01772-09 (visited on 07/15/2025).

[20] D. Mikkelsen et al. “Influence of different carbon sources on bacterial cellulose production by Gluconacetobacter xylinus strain ATCC 53524”. eng. In: *Journal of Applied Microbiology* 107.2 (Aug. 2009), pp. 576–583. ISSN: 1365-2672. DOI: 10.1111/j.1365-2672.2009.04226.x.

[21] Fabian Mittermeier et al. “Artificial microbial consortia for bioproduction processes”. en. In: *Engineering in Life Sciences* 23.1 (2023). _eprint: https://analyticalsciencejournals.onlinelibrary.wiley.com/doi/pdf/10.1002/elsc.202100152, e2100152. ISSN: 1618-2863. DOI: 10.1002/elsc.202100152. URL: https://onlinelibrary.wiley.com/doi/abs/10.1002/elsc.202100152 (visited on 12/10/2025).

[22] Pedro Montenegro-Silva et al. “Enhanced bacterial cellulose production in Komagataeibacter sucrofermentans: impact of different PQQ-dependent dehydrogenase knockouts and ethanol supplementation”. In: *Biotechnology for Biofuels and Bioproducts* 17 (Feb. 2024), p. 35. ISSN: 2731-3654. DOI: 10.1186/s13068-024-02482-9. URL: https://www.ncbi.nlm.nih.gov/pmc/articles/PMC10902950/ (visited on 04/16/2025).

[23] Francisco X. Nascimento et al. “Functional and genomic characterization of *Komagataeibacter uvaceti* FXV3, a multiple stress resistant bacterium producing increased levels of cellulose”. In: *Biotechnology Reports* 30 (June 2021), e00606. ISSN: 2215-017X. DOI: 10.1016/j.btre.2021.e00606. URL: https://www.sciencedirect.com/science/article/pii/S2215017X21000229 (visited on 11/19/2025).

[24] Clara Navarrete, Jens Nielsen, and Verena Siewers. “Enhanced ethanol production and reduced glycerol formation in fps1 mutants of Saccharomyces cerevisiae engineered for improved redox balancing”. In: *AMB Express* 4.1 (Dec. 2014), p. 86. ISSN: 2191-0855. DOI: 10.1186/s13568-014-0086-z. URL: https://doi.org/10.1186/s13568-014-0086-z (visited on 04/16/2025).

[25] Thais Jardim Oliveira et al. “Evolution of Bacterial Cellulose in Cosmetic Applications: An Updated Systematic Review”. en. In: *Molecules* 27.23 (Jan. 2022). Publisher: Multidisciplinary Digital Publishing Institute, p. 8341. ISSN: 1420-3049. DOI: 10.3390/molecules27238341. URL: https://www.mdpi.com/1420-3049/27/23/8341 (visited on 12/04/2025).

[26] Pelin Özkaya, Seval Dağbağlı, and Müge Uyarcan. “Utilization of food wastes in production of bacterial cellulose”. In: *Ege Univ. Ziraat Fak. Derg.* 60.4 (2023), pp. 737–749. DOI: 10.20289/zfdergi.1350359. URL: https://doi.org/10.20289/zfdergi.1350359.

[27] Jacob D. Palmer and Kevin R. Foster. “Bacterial species rarely work together”. In: *Science* 376.6593 (2022), pp. 581–582. DOI: 10.1126/science.abn5093. eprint: https://www.science.org/doi/pdf/10.1126/science.abn5093. URL: https://www.science.org/doi/abs/10.1126/science.abn5093.

[28] J. K. Park, S. H. Hyun, and J. Y. Jung. “Conversion of G. hansenii PJK into non-cellulose-producing mutants according to the culture condition”. In: *Biotechnology and Bioprocess Engineering* 9.4 (2004), pp. 383–388. DOI: 10.1007/BF02933062. URL: https://doi.org/10.1007/BF02933062.

[29] J. K. Park, J. Y. Jung, and Y. H. Park. “Cellulose production by Gluconacetobacter hansenii in a medium containing ethanol”. In: *Biotechnology Letters* 25.25 (2003), pp. 2055–2059. DOI: 10.1023/B:BILE.0000007065.63682.18. URL: https://doi.org/10.1023/B:BILE.0000007065.63682.18.

[30] T. A. H. Puvvada. “ODE-based mathematical modelling of yeast-bacteria consortium for the production of bacterial cellulose”. English. Student report, MSc thesis, online resource (IV, 29 pages). Master’s thesis. Wageningen University & Research, Systems and Synthetic Biology, 2025.

[31] R. Rathinamoorthy and T. Kiruba. “Bacterial Cellulose—A Sustainable Alternative Material for Footwear and Leather Products”. en. In: *Leather and Footwear Sustainability: Manufacturing, Supply Chain, and Product Level Issues*. Ed. by Subramanian Senthilkannan Muthu. Singapore: Springer, 2020, pp. 91–121. ISBN: 978-981-15-6296-9. DOI: 10.1007/978-981-15-6296-9_5. URL: https://doi.org/10.1007/978-981-15-6296-9_5 (visited on 12/04/2025).

[32] Cesar Augusto Roque-Borda et al. “Cellulose from bacteria as a delivery system for improved treatment of infectious diseases: A review of updates and prospects”. In: *International Journal of Biological Macromolecules* 277.Pt 1 (2024), p. 133831. DOI: 10.1016/j.ijbiomac.2024.133831. URL: https://doi.org/10.1016/j.ijbiomac.2024.133831.

[33] Baljeet Singh Saharan et al. "Biopolymer and polymer precursor production by microorganisms: applications and future prospects". en. In: *Journal of Chemical Technology & Biotechnology* 99.1 (2024). _eprint: https://scijournals.onlinelibrary.wiley.com/doi/pdf/10.1002/jctb.7524, pp. 17–30. ISSN: 1097-4660. DOI: 10.1002/jctb.7524. URL: https://onlinelibrary.wiley.com/doi/abs/10.1002/jctb.7524 (visited on 12/04/2025).

[34] Boris Sakschewski et al. *Planetary Health Check 2025: A Scientific Assessment of the State of the Planet*. en. Tech. rep. Artwork Size: 144 pages, 22 MB Medium: application/pdf Publication Title: Planetary Boundaries Science (PBScience). Potsdam Institute for Climate Impact Research (PIK), Sept. 2025, 144 pages, 22 MB. DOI: 10.48485/PIK.2025.017. URL: https://publications.pik-potsdam.de/pubman/item/item_32589 (visited on 12/04/2025).

[35] Vudata Subhashini and Rajesh Paneti. "Recent Advances in Waste-Derived Biopolymers: A Comprehensive Review". en. In: *International Journal of Scientific Research and Technology* (Aug. 2025). Publisher: IJSRT Journal. ISSN: 2394-7063. DOI: 10.5281/zenodo.17013406. URL: https://www.ijsrtjournal.com/article/Recent+Advances+in+WasteDerived+Biopolymers+A+Comprehensive+Review (visited on 12/09/2025).

[36] Pornchanok Taweecheep et al. "Superfine bacterial nanocellulose produced by reverse mutations in the *bcsC* gene during adaptive breeding of *Komagataeibacter oboediens*". In: *Carbohydrate Polymers* 226 (2019), p. 115243. ISSN: 0144-8617. DOI: 10.1016/j.carbpol.2019.115243. URL: https://doi.org/10.1016/j.carbpol.2019.115243.

[37] W. Treesuppharat et al. "Synthesis and characterization of bacterial cellulose and gelatin-based hydrogel composites for drug-delivery systems". In: *Biotechnology Reports* 15 (Sept. 2017), pp. 84–91. ISSN: 2215-017X. DOI: 10.1016/j.btre.2017.07.002. URL: https://www.sciencedirect.com/science/article/pii/S2215017X17300735 (visited on 12/04/2025).

[38] Zhongjuan Wang et al. "Applications of bacterial cellulose in the food industry and its health-promoting potential". In: *Food Chemistry* 464 (Feb. 2025), p. 141763. ISSN: 0308-8146. DOI: 10.1016/j.foodchem.2024.141763. URL: https://www.sciencedirect.com/science/article/pii/S0308814624034137 (visited on 12/04/2025).

[39] Melanie Wijsman et al. "A toolkit for rapid CRISPR-SpCas9 assisted construction of hexose-transport-deficient Saccharomyces cerevisiae strains". In: *FEMS Yeast Research* 19.1 (Jan. 2019), foy107. ISSN: 1567-1356. DOI: 10.1093/femsyr/foy107. URL: https://doi.org/10.1093/femsyr/foy107 (visited on 04/25/2025).

[40] Aqiang Wu et al. "Single-Ion Conductive Bacterial Cellulose Membrane Towards High Performance Lithium-Oxygen Batteries". en. In: *Battery Energy* 4.6 (2025). _eprint: https://onlinelibrary.wiley.com/doi/pdf/10.1002/bte2.20250001, e70027. ISSN: 2768-1696. DOI: 10.1002/bte2.20250001. URL: https:

//onlinelibrary.wiley.com/doi/abs/10.1002/bte2.20250001 (visited on 12/04/2025).

[41] Shunji Yunoki et al. "Role of Ethanol in Improvement of Bacterial Cellulose Production: Analysis Using 13C-Labeled Carbon Sources". In: *Food Science and Technology Research* 10.3 (2004), pp. 307–313. DOI: 10.3136/fstr.10.307.

[42] Heng Zhang et al. "Effect of Culture Conditions on Cellulose Production by a Komagataeibacter xylinus Strain". In: *Macromolecular Bioscience* 22.6 (2022), p. 2100476. DOI: https://doi.org/10.1002/mabi.202100476. eprint: https://onlinelibrary.wiley.com/doi/pdf/10.1002/mabi.202100476. URL: https://onlinelibrary.wiley.com/doi/abs/10.1002/mabi.202100476.

[43] Chunyan Zhong. "Industrial-scale production and applications of bacterial cellulose". In: *Frontiers in Bioengineering and Biotechnology* 8 (2020), p. 605374. DOI: 10.3389/fbioe.2020.605374. URL: https://doi.org/10.3389/fbioe.2020.605374.

[44] Hengrui Zhou et al. "One-pot production of colored bacterial cellulose". English. In: *Trends in Biotechnology* 0.0 (Nov. 2025). Publisher: Elsevier. ISSN: 0167-7799, 1879-3096. DOI: 10.1016/j.tibtech.2025.09.019. URL: https://www.cell.com/trends/biotechnology/abstract/S0167-7799(25)00407-X (visited on 12/01/2025).

7 Appendix

7.1 History of the strain *Saccharomyces cerevisiae* IMX1812

Table 1. Strains used in this study.

Name	Relevant genotype	Parental strain	Origin
CEN.PK113-7D	MATa *URA3 TRP1 LEU2 HIS3*		(Entian and Kötter 2
CEN.PK2-1C	MATa *ura3-52 trp1-1 his3Δ*		(Entian and Kötter 2
CEN.PK122	*MATa/MATα*		(Entian and Kötter 2
EBY.VW4000	MATa *ura3-52 trp1-1 leu2-3,112 his3Δ hxt13Δ::loxP hxt15Δ::loxP hxt16Δ::loxP hxt14Δ::loxP hxt12Δ::loxP hxt9Δ::loxP hxt11Δ::loxP hxt10Δ::loxP hxt8Δ::loxP hxt4-1-5Δ::loxP hxt2Δ::loxP hxt3-6-7Δ::loxP gal2Δ stl1Δ::loxP agt1Δ::loxP mph2(ydl247w)Δ::loxP mph3(yjr160c)Δ::loxP*	CEN.PK2-1C	(Wieczorke *et al.* 199
IMX672	MATa *ura3-52 trp1-1 leu2-3,112 his3Δ can1Δ::Spcas9-natNT2*	CEN.PK2-1C	(Mans *et al.* 2015)
IMX1521	MATa *ura3-52 trp1-1 leu2-3,112 his3Δ can1Δ::Spcas9-natNT2 gal2Δ hxt4-1-5Δ hxt3-6-7Δ::ars4 hxt8Δ hxt14Δ*	IMX672	This study
IMX1541	MATa *ura3-52 trp1-1 leu2-3,112 his3Δ can1Δ::Spcas9-natNT2 gal2Δ hxt4-1-5Δ hxt3-6-7Δ::ars4 hxt8Δ hxt14Δ hxt2Δ hxt9Δ hxt10Δ hxt12Δ hxt13Δ hxt15Δ hxt16Δ*	IMX1521	This study
IMX1812	MATa *ura3-52 trp1-1 leu2-3,112 his3Δ can1Δ::Spcas9-natNT2 gal2Δ hxt4-1-5Δ hxt3-6-7Δ::ars4 hxt8Δ hxt14Δ hxt2Δ hxt9Δ hxt10Δ hxt11Δ hxt12Δ hxt13Δ hxt15Δ hxt16Δ mph2(ydl247w)Δ mph3(yjr160c)Δ mal11Δ stl1Δ*	IMX1541	This study

Figure A1: **History of the hexose-transport deficient *S.cerevisiae* IMX1812** Figure reproduced from Wijsman et al. (2019). [39].

7.2 Maximum theoretical concentrations of metabolites in the coculture

7.2.1 From glucose by *K.sucrofermentans*

In acetic acid bacteria, acetate can be produced via at least two main routes:

Route 1: Ethanol oxidation in the periplasm

1. Ethanol is first oxidised to acetaldehyde by an alcohol dehydrogenase (ADH):
$$\text{ethanol} \xrightarrow{\text{ADH}} \text{acetaldehyde}$$

2. Acetaldehyde is then further oxidised to acetate by an aldehyde dehydrogenase (ALDH):
$$\text{acetaldehyde} \xrightarrow{\text{ALDH}} \text{acetate}$$

Route 2: Glucose to acetate via acetyl-CoA Glucose can also be converted to acetate via glycolysis, pyruvate dehydrogenase (PDH) and acetate-forming enzymes (e.g. phosphotransacetylase/acetate kinase, Pta/AckA):

$$\text{glucose} \;\rightarrow\; \text{glycolysis/PDH/TCA} \;\rightarrow\; \text{acetyl-CoA} \;\rightarrow\; \text{acetate}.$$

Stoichiometric maximum yield of acetate from glucose: A simplified overall carbon balance for glycolysis plus PDH is:

$$\mathrm{C_6H_{12}O_6} \;\rightarrow\; 2\,\text{acetyl-CoA} + 2\,\mathrm{CO_2}. \tag{3}$$

Each acetyl-CoA (2C) can then be converted to acetate (2C), for example via the Pta/AckA pathway:

$$\text{acetyl-CoA} \;\rightarrow\; \text{acetate}. \tag{4}$$

Per mole of glucose, this gives:

$$1\,\text{glucose} \;\rightarrow\; 2\,\text{acetate} + 2\,\mathrm{CO_2}. \tag{5}$$

Thus, the **maximum molar yield** is:

$$Y_{\mathrm{Ac/Glc,max}} = \frac{2 \text{ mol acetate}}{1 \text{ mol glucose}}. \tag{6}$$

Conversion to g/g yield: Approximate molar masses:

- Glucose: $M_{\mathrm{Glc}} = 180.16\ \mathrm{g\,mol^{-1}}$
- Acetic acid: $M_{\mathrm{Ac}} = 60.05\ \mathrm{g\,mol^{-1}}$

Mass of acetate produced from 1 mol glucose at the theoretical maximum:

$$m_{\mathrm{Ac}} = 2 \times 60.05 \text{ g} = 120.10 \text{ g}. \tag{7}$$

Yield in g/g:

$$Y_{\mathrm{Ac/Glc,max}} = \frac{120.10 \text{ g acetate}}{180.16 \text{ g glucose}} \approx 0.667 \text{ g acetate g}^{-1} \text{ glucose}. \tag{8}$$

Thus, the theoretical maximum yield is:

$$Y_{\mathrm{Ac/Glc,max}} \approx 0.67 \text{ g g}^{-1}. \tag{9}$$

The carbon yield is the same fraction, since four of the six carbon atoms in glucose end up in acetate:

$$Y_{\mathrm{C,Ac/Glc}} = \frac{4 \text{ C}}{6 \text{ C}} = \frac{4}{6} \approx 0.667 \text{ C-mol C-mol}^{-1}. \tag{10}$$

Application to 20 g L^{-1} glucose: For an initial concentration of 20 g L^{-1} glucose, the theoretical maximum acetate concentration is:

$$c_{\mathrm{Ac,max}} = 20 \text{ g L}^{-1} \times 0.667 \ \frac{\text{g acetate}}{\text{g glucose}} \tag{11}$$

$$\approx 13.3 \text{ g L}^{-1} \text{ acetate}. \tag{12}$$

In molar terms:

$$n_{\mathrm{Glc}} = \frac{20 \text{ g L}^{-1}}{180.16 \text{ g mol}^{-1}} \approx 0.111 \text{ mol L}^{-1}, \tag{13}$$

$$n_{\mathrm{Ac,max}} = 2 \times n_{\mathrm{Glc}} \approx 0.222 \text{ mol L}^{-1}, \tag{14}$$

$$c_{\mathrm{Ac,max}} = 0.222 \text{ mol L}^{-1} \times 60.05 \text{ g mol}^{-1} \approx 13.3 \text{ g L}^{-1}. \tag{15}$$

Assuming ≈ 1 kg of solution per litre, this corresponds to:

$$\frac{13.3 \text{ g}}{1000 \text{ g}} \times 100\% \approx 1.33\% \text{ (w/v)} \tag{16}$$

as an upper-bound estimate for acetate concentration in the coculture.

Theoretical gluconate concentrations: A study reported a gluconate yield of approximately 0.39 g gluconate per g glucose [8]. Applying this yield to 20 $\mathrm{g\,L^{-1}}$ glucose gives:

$$c_{\mathrm{Glu}} = 20\ \mathrm{g\,L^{-1}} \times 0.39\ \frac{\text{g gluconate}}{\text{g glucose}} \tag{17}$$

$$\approx 7.8\ \mathrm{g\,L^{-1}}\ \text{gluconate.} \tag{18}$$

Expressed as a percentage (w/v), this is:

$$\frac{7.8\ \mathrm{g}}{1000\ \mathrm{g}} \times 100\% \approx 0.78\%, \tag{19}$$

i.e. around 0.8% gluconate in the medium under these theoretical conditions.

7.2.2 From maltose by fermentative *S.cerevisiae*

Theoretical yield of ethanol produced from maltose by fermentative *S.cerevisiae*: For fermentative *S. cerevisiae*, classical alcoholic fermentation of glucose is:

$$\mathrm{C_6H_{12}O_6} \ \rightarrow\ 2\,\mathrm{C_2H_5OH} + 2\,\mathrm{CO_2}. \tag{20}$$

Using approximate molar masses

$$M_{\mathrm{Glc}} = 180.16\ \mathrm{g\,mol^{-1}}, \quad M_{\mathrm{EtOH}} = 46.07\ \mathrm{g\,mol^{-1}},$$

the maximum mass yield of ethanol from glucose is:

$$Y_{\mathrm{EtOH/Glc,max}} = \frac{2 \times M_{\mathrm{EtOH}}}{M_{\mathrm{Glc}}} = \frac{2 \times 46.07}{180.16} \approx 0.511\ \text{g ethanol}\,\mathrm{g^{-1}}\ \text{glucose.} \tag{21}$$

For maltose (a disaccharide), the stoichiometry is:

$$\mathrm{C_{12}H_{22}O_{11}} \ \rightarrow\ 2\,\mathrm{C_6H_{12}O_6} \ \rightarrow\ 4\,\mathrm{C_2H_5OH} + 4\,\mathrm{CO_2}. \tag{22}$$

With $M_{\mathrm{Malt}} \approx 342.30\ \mathrm{g\,mol^{-1}}$, the corresponding theoretical yield from maltose is:

$$Y_{\mathrm{EtOH/Malt,max}} = \frac{4 \times M_{\mathrm{EtOH}}}{M_{\mathrm{Malt}}} = \frac{4 \times 46.07}{342.30} \approx 0.538\ \text{g ethanol}\,\mathrm{g^{-1}}\ \text{maltose.} \tag{23}$$

This is consistent with the glucose-based yield ($0.511\ \mathrm{g\,g^{-1}}$) when the difference in molar mass between glucose and maltose is taken into account.

Application to 6.8 g L^{-1} maltose in a 100 mL coculture In the coculture experiments, the initial maltose concentration was

$$c_{\mathrm{Malt}} = 6.8\ \mathrm{g\,L^{-1}}.$$

For a culture volume of $V = 0.100$ L (100 mL), the total maltose mass is:

$$m_{\mathrm{Malt}} = c_{\mathrm{Malt}} \times V = 6.8\ \mathrm{g\,L^{-1}} \times 0.100\ \mathrm{L} = 0.68\ \mathrm{g}. \tag{24}$$

Using the theoretical yield $Y_{\mathrm{EtOH/Malt,max}} \approx 0.538\ \mathrm{g\,g^{-1}}$, the maximum amount of ethanol that could be produced from this maltose is:

$$m_{\mathrm{EtOH,max}} = m_{\mathrm{Malt}} \times Y_{\mathrm{EtOH/Malt,max}} \tag{25}$$

$$\approx 0.68\ \mathrm{g} \times 0.538\ \frac{\mathrm{g\ ethanol}}{\mathrm{g\ maltose}} \tag{26}$$

$$\approx 0.37\ \mathrm{g\ ethanol}. \tag{27}$$

Expressed as a concentration:

$$c_{\mathrm{EtOH,max}} = \frac{m_{\mathrm{EtOH,max}}}{V} \approx \frac{0.37\ \mathrm{g}}{0.100\ \mathrm{L}} \approx 3.7\ \mathrm{g\,L^{-1}}. \tag{28}$$

Assuming a broth density of approximately 1 kg L^{-1} and an ethanol density of 0.789 g mL^{-1}, this corresponds to approximately 3.7 g L^{-1} ethanol (0.37% w/v), i.e. about 4.7 mL ethanol per litre, or 0.47% v/v.

7.3 96 well-plate layouts for the growth kinetics experiments

7.3.1 96 Well-plate layout for *K.sucrofermentans* and WT *S.cerevisiae*

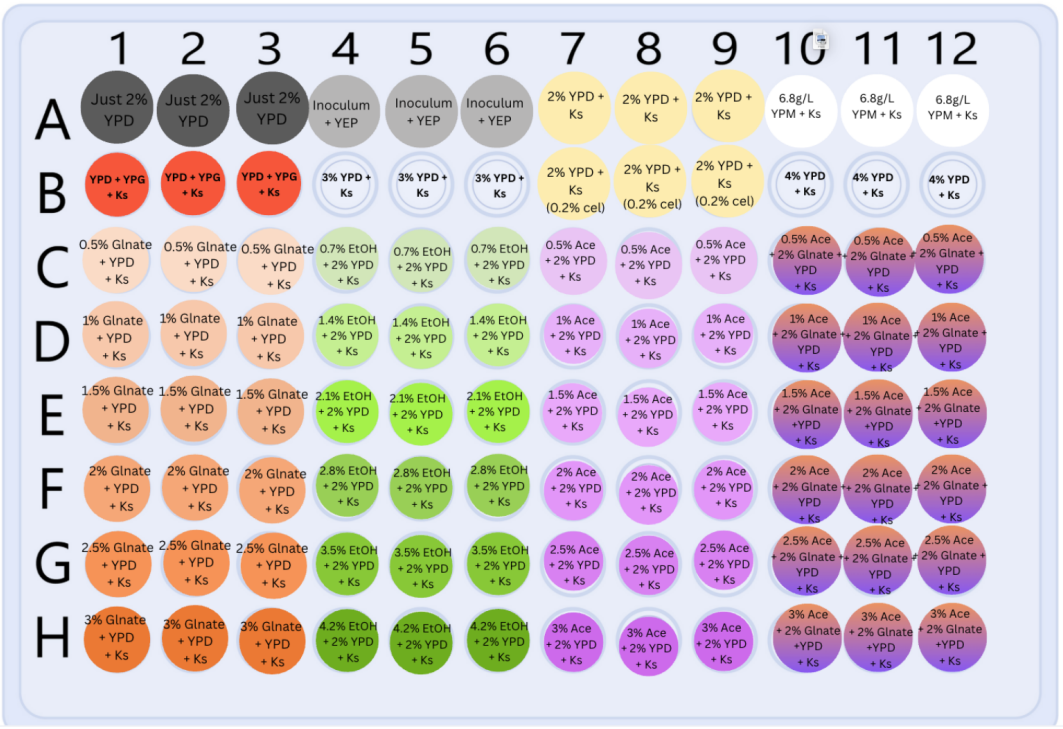

Figure A2: **96 WP layout used for both *K.sucrofermentans* and *S.cerevisiae* CENPK113-7D (WT) and Δ WT**

7.3.2 96 Well-plate layout for the strain *S.cerevisiae* IMX1812 ρ

Figure A3: **96 WP layout used for the strain *S.cerevisiae* IMX1812 ρ**

The corresponding percentages conversion table:

Ethanol (% v/v)	Ethanol (mM)	Sodium Acetate (% w/v)	Sodium Acetate (mM)	Sodium Gluconate (% w/v)	Sodium Gluconate (mM)
0.8	137.00889950075972	0.5	60.953309764720224	0.7	32.08948381773173
1.6	274.01779900151945	1.0	121.90661952944045	1.4	64.17896763546347
2.4000000000000004	411.0266985022792	1.5	182.85992929416068	2.0999999999999996	96.26845145319518
3.2	548.0355980030389	2.0	243.8132390588809	2.8	128.35793527092693
4.0	685.0444975037985	2.5	304.7665488236011	3.5	160.44741908865868
4.800000000000001	822.0533970045584	3.0	365.71985858832136	4.199999999999999	192.53690290639037

Figure A4: **Table to convert mM to percentages**

7.4 Adapting the protocol for the coculture for *S.cerevisiae* Δmitochondria from Gilbert et al.

Table 2: Specific growth rates and doubling times of wild-type (WT) and mitochondrial-deficient (ρ^-) *S. cerevisiae* used to derive the scaling factor for adapting coculture conditions.

Strain	$\boldsymbol{\mu_{avg}}$ (h^{-1}) ± SD	**Doubling time (h)**
WT	0.455 ± 0.0739	1.56
ρ^- (Δmito)	0.283 ± 0.0621	2.54
WT/ρ^- ratio in μ: 1.61		
ρ^-/WT ratio in doubling time: 1.63		

The 1.6 ratio was used to scale preculture duration, inoculum OD and inoculum concentration when adapting WT coculture protocol from Gilbert et al. (2021) WT to the fermentative Δmitochondria strain [11] .

7.5 HPLC analysis calibration curves and results

7.5.1 The calibration curves

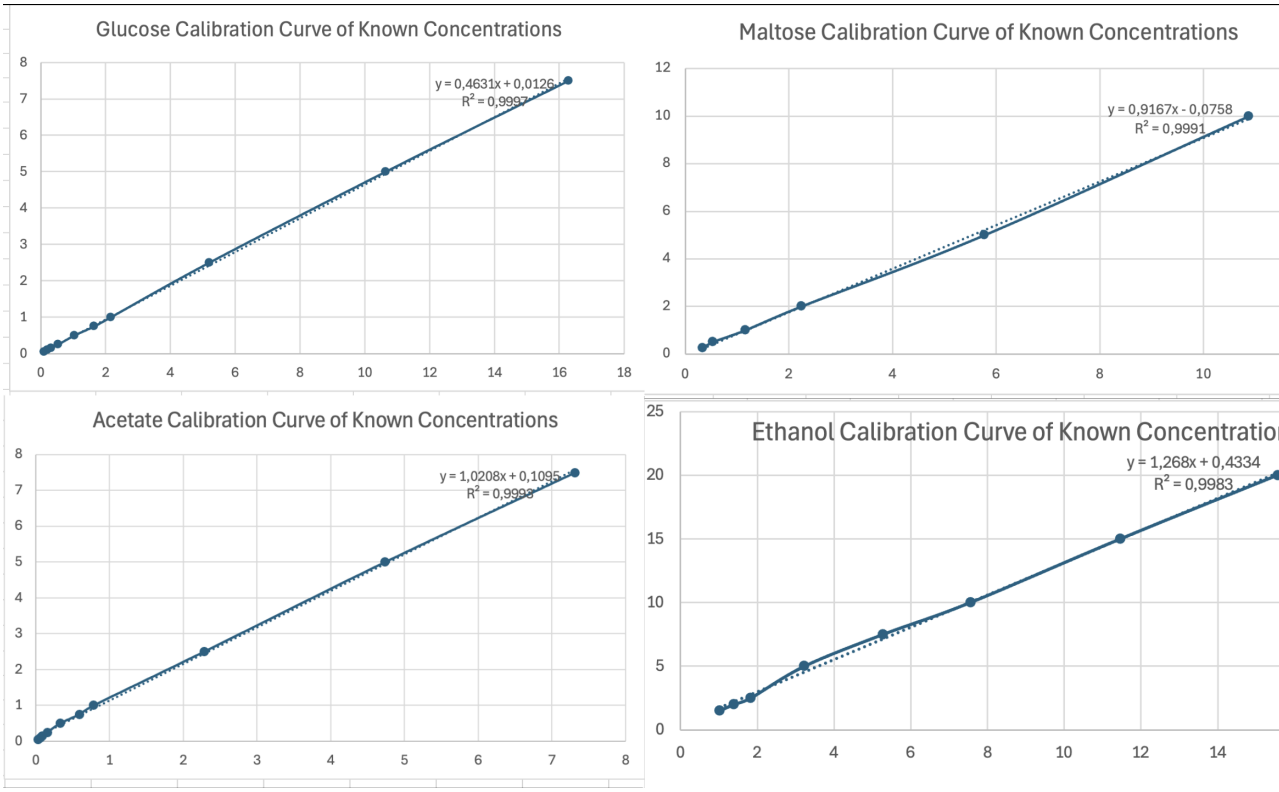

Figure A5: **Calibration curves for glucose, maltose, ethanol and acetate obtained from known standard concentrations of 20 (for glucose and maltose), 10, 5, 2, 1, 0.5, and 0.25 g/L**

7.5.2 HPLC Results

Table 3: HPLC-derived metabolite concentrations (g/L) at the start and end of the cultures.

Sample	Timepoint	Metabolite	Rep 1	Rep 2	Mean	SD
Ks	Start	maltose	0.496221	0.748405	0.622313	0.178321
Ks	Start	glucose	11.95641	9.393431	10.67492	1.812301
Ks	Start	acetate	0.1095	0.1095	0.1095	0.000000
Ks	Start	ethanol	0.4334	0.4334	0.4334	0.000000
Ks	End	maltose	0.264204	0.206635	0.235420	0.040707
Ks	End	glucose	0.0879	0.068404	0.078152	0.013786
Ks	End	acetate	2.132419	2.26839	2.200405	0.096146
Ks	End	ethanol	3.710419	1.902124	2.806272	1.278658
Coculture	Start	maltose	8.533021	9.46173	8.997376	0.656696
Coculture	Start	glucose	11.55416	13.78751	12.67084	1.579214
Coculture	Start	acetate	0.1095	0.1095	0.1095	0.000000
Coculture	Start	ethanol	0.4334	0.4334	0.4334	0.000000
Coculture	End	maltose	0.231845	0.304172	0.268008	0.051143
Coculture	End	glucose	0.031031	0.049787	0.040409	0.013262
Coculture	End	acetate	2.863006	2.914985	2.888985	0.036740
Coculture	End	ethanol	1.350798	1.651821	1.501310	0.212856

7.6 Replicates removed due to Richard's fits

The Richard's fit files are provided as supplementary figures.

For the graphs showing the growth rate of *K.sucrofermentans* on ethanol, gluconate, acetate, and acetate and gluconate

- 1% acetate condition was excluded since replicates (D7D8D9, check Richards' fit of these wells) were unreliable. All replicates reached unrealistically high carrying capacity ODs and one of them did not show growth until the 10th hour.

-3% acetate condition was excluded since replicates (H7H8H9, check Richards' fit of these wells) were unreliable. All replicates reached unrealistically high carrying capacity ODs and one of them did not show growth until around the 17th hour.

Table 4: Endpoint pH of duplicates (A and B) for *K. sucrofermentans* (Ks) monocultures and coculture. Standard deviations (SD) are calculated as sample SD ($n = 2$; equivalent to Excel `STDEV.S`).

Condition	Duplicate A	Duplicate B	Mean pH	SD
K. sucrofermentans monoculture (Ks)	3.93	4.03	3.98	0.071
Coculture	4.00	3.85	3.925	0.106

7.7 Coculture 1 pH after 4 days of cultivation

7.8 Theoretical estimation of undissociated weak-acid fractions at pH 4.0

For a monoprotic weak acid HA in equilibrium with its conjugate base A^-, the Henderson–Hasselbalch equation relates the pH to the acid dissociation constant:

$$\mathrm{pH} = \mathrm{p}K_\mathrm{a} + \log_{10}\left(\frac{[\mathrm{A}^-]}{[\mathrm{HA}]}\right). \tag{29}$$

Rearranging gives the ratio between base and acid:

$$\frac{[\mathrm{A}^-]}{[\mathrm{HA}]} = 10^{\mathrm{pH}-\mathrm{p}K_\mathrm{a}}. \tag{30}$$

The fraction of the total acid present in the undissociated form (HA) is then

$$f_\mathrm{HA} = \frac{[\mathrm{HA}]}{[\mathrm{HA}] + [\mathrm{A}^-]} = \frac{1}{1 + 10^{\mathrm{pH}-\mathrm{p}K_\mathrm{a}}}, \tag{31}$$

and the fraction present as the conjugate base (A^-) is $f_{\mathrm{A}^-} = 1 - f_\mathrm{HA}$.

Acetic acid at pH 4.0

Using $\mathrm{p}K_\mathrm{a} = 4.76$ for acetic acid and pH = 4.00:

$$f_\mathrm{HA,Ac} = \frac{1}{1 + 10^{\mathrm{pH}-\mathrm{p}K_\mathrm{a}}} = \frac{1}{1 + 10^{4.00-4.76}} \tag{32}$$

$$= \frac{1}{1 + 10^{-0.76}} = \frac{1}{1 + 0.1738} \approx 0.8519. \tag{33}$$

Thus, at pH 4.0:

$$f_{\mathrm{HA,Ac}} \approx 0.8519 \quad \text{(undissociated acetic acid, 85.2\%)} \tag{34}$$

$$f_{\mathrm{A^-,Ac}} = 1 - f_{\mathrm{HA,Ac}} \approx 0.1481 \quad \text{(acetate, 14.8\%)}. \tag{35}$$

Gluconic acid at pH 4.0

Using $\mathrm{p}K_\mathrm{a} = 3.70$ for gluconic acid and $\mathrm{pH} = 4.00$:

$$f_{\mathrm{HA,Glu}} = \frac{1}{1 + 10^{\mathrm{pH}-\mathrm{p}K_\mathrm{a}}} = \frac{1}{1 + 10^{4.00-3.70}} \tag{36}$$

$$= \frac{1}{1 + 10^{0.30}} = \frac{1}{1 + 1.9953} \approx 0.3339. \tag{37}$$

Thus, at pH 4.0:

$$f_{\mathrm{HA,Glu}} \approx 0.3339 \quad \text{(undissociated gluconic acid, 33.4\%)} \tag{38}$$

$$f_{\mathrm{A^-,Glu}} = 1 - f_{\mathrm{HA,Glu}} \approx 0.6661 \quad \text{(gluconate, 66.6\%)}. \tag{39}$$